

Dynamic trafficking and turnover of Jam-C is essential for endothelial cell migration

Katja B. Kostelnik¹¥, Amy Barker¹¥, Christopher Schultz¹, Vinothini Rajeeve², Ian J. White³, Michel Aurrand-Lions⁴, Sussan Nourshargh¹, Pedro Cutillas² and Thomas D. Nightingale¹◊

1. Centre for Microvascular Research, William Harvey Research Institute, Barts and the London School of Medicine and Dentistry, Queen Mary University of London, UK.

2. Cell Signalling & Proteomics Group, Barts Cancer Institute, Queen Mary University of London, London, UK.

3. MRC Laboratory of Molecular Cell Biology, University College London, London, UK.

4. Aix Marseille University, CNRS, INSERM, Institut Paoli-Calmettes, CRCM, Marseille, France

¥ These authors contributed equally

◊ Author for correspondence: t.nightingale@qmul.ac.uk

Abstract

Junctional complexes between endothelial cells form a dynamic barrier that hinder passive diffusion of blood constituents into interstitial tissues. Re-modelling of junctions is an essential process during leukocyte trafficking, vascular permeability and angiogenesis. However, for many junctional proteins the mechanisms of junctional remodelling have yet to be determined. Here we used receptor mutagenesis, HRP and APEX-2 proximity labelling, alongside light and electron microscopy, to map the intracellular trafficking routes of junctional adhesion molecule-C (Jam-C). We found that Jam-C co-traffics with receptors associated with changes in permeability, such as VE-Cadherin, NRP-1 and 2, but not with junctional proteins associated with the transmigration of leukocytes. Dynamic Jam-C trafficking and degradation is necessary for junctional remodelling during cell migration and angiogenesis. By identifying new trafficking machinery we show that a key point of regulation is the ubiquitylation of Jam-C by the E3 ligase CBL, this controls the rate of recycling versus lysosomal degradation.

30 Introduction

31 Endothelial cells exist as a monolayer that lines the blood vasculature and as such they
32 present a discrete barrier to the cellular and molecular components of blood. This includes
33 ions, small and large proteins, platelets and leukocytes¹. The endothelium also plays a crucial
34 role in responding to a pathogenic infection or tissue injury; both in the initial recruitment of
35 leukocytes to the appropriate site², and in subsequent tissue repair and angiogenesis³.
36 Endothelial dysfunction can predispose the vessel wall to leukocyte adhesion, platelet
37 activation, oxidative stress, thrombosis, coagulation and chronic inflammation leading to the
38 pathogenesis of numerous cardiovascular diseases⁴.

39

40 Essential to the establishment of the endothelial monolayer are the protein complexes
41 between adjacent cells that create junctions. Junctions are dynamic and are remodelled to
42 control processes such as cell permeability¹ and cell migration⁵, and a subset of junctional
43 proteins also control leukocyte transmigration². This subset includes molecules such as VE-
44 Cadherin, PECAM-1 (CD31), CD99, endothelial cell-selective adhesion molecule (ESAM),
45 ICAM-1 and -2 and the junctional adhesion molecule (Jam) family of proteins (Jam-A, -B and -
46 C)^{2, 6}. These proteins engage in homophilic and heterophilic interactions with neighbouring
47 cells or with transmigrating leukocytes. Control of these interactions determines the stability
48 of the junctions and/or provides unligated receptor for the movement of transmigrating
49 leukocytes^{2, 7}. For some receptors that are directly required for leukocyte transmigration
50 (such as Jam-A and PECAM-1) this is a well characterised process regulated by a combination
51 of phosphorylation, proteolytic cleavage and intracellular trafficking. However, for other
52 receptors such as Jam-C almost nothing is known about the molecular control of receptor
53 trafficking and its importance to function.

54

55 Jam-C is a type-1 integral membrane protein of the Ig superfamily that mediates numerous
56 endothelial cell functions such as leukocyte trans-endothelial cell migration⁸⁻¹², angiogenesis
57 and vascular permeability¹³⁻¹⁶. However, there is a marked difference in the function of Jam-
58 C compared to other endothelial junctional receptors. Rather than directly inhibiting
59 leukocyte transmigration, inhibition of Jam-C by genetic means or using blocking antibodies
60 changes the mode of transmigration^{8, 11, 17, 18}. In Jam-C-deficient endothelial cells, leukocytes
61 breach the endothelial barrier and then reverse, transmigrating back into the vessel lumen,

62 reducing the overall efficiency of leukocyte traffic. Further, unlike Jam-A, Jam-C surface
63 expression favours changes in permeability following stimulation with thrombin, VEGF or
64 histamine by inhibiting the activation of the small GTPase Rap-1 and by activating actomyosin
65 function¹⁵. Given these functional differences it is likely for the regulation of Jam-C to be
66 similarly diverse. Together, the broad functional roles of Jam-C in inflammation and vascular
67 biology is illustrated through its involvement in multiple inflammatory disease states such as
68 arthritis¹⁹, peritonitis⁹, acute pancreatitis^{18, 20}, ischemia reperfusion injury^{10, 11}, pulmonary
69 inflammation^{21, 22} and atherosclerosis²³⁻²⁵.

70

71 Whilst little is known about the molecular mechanisms of Jam-C trafficking, current evidence
72 indicates an important role for such a phenomenon in regulating Jam-C function. Firstly, in
73 cultured macro and microvascular endothelial cells Jam-C can be redistributed in a stimulus-
74 dependent manner^{13, 15, 26}; activation of endothelial cells with thrombin, VEGF or histamine
75 increases localisation of Jam-C at the cell surface. Secondly, analysis of inflamed murine
76 tissues by electron microscopy showed labelling of the extracellular domain of Jam-C within
77 vesicles, at the cell surface and at junctional regions of endothelial cells. Importantly,
78 distribution of Jam-C was altered within these sites following an inflammatory stimulus
79 (ischemia/reperfusion injury), resulting in a change in the levels of vesicular protein vs.
80 junctional and cell surface protein^{10, 11}. Finally, enhanced levels of Jam-C have been observed
81 in atherosclerosis and rheumatoid arthritis, some of which likely reflect changes in
82 intracellular trafficking^{19, 24}.

83 Collectively current evidence suggests a causal link between redistribution of intracellular
84 Jam-C and physiological and pathological processes involving opening of endothelial cell
85 junctions. To directly address this hypothesis, we investigated the mechanisms underlying
86 Jam-C redistribution and trafficking using wild-type and mutant variants of this receptor and
87 a combination of light and electron microscopy. Furthermore, to identify co-trafficked cell
88 surface receptors and trafficking machinery involved in Jam-C internalisation and subcellular
89 localisation, we developed novel proximity labelling mass spectrometry approaches. By
90 perturbing the newly identified pathways of Jam-C re-distribution, and using mutant variants
91 of this receptors, we show that a key point of regulation is the ubiquitylation of Jam-C by the
92 E3 ligase CBL, this regulates the rate of recycling versus lysosomal degradation.

93

94 Methods

95 Constructs and cloning

96 pRK5-HA-Ubiquitin-WT was a gift from Ted Dawson (Addgene plasmid # 17608). Murine Jam-
97 C-GFPout and Jam-C-GFPout Δ PDZ have been described previously²⁷. To generate Murine
98 Jam-C-HRPout, HRP was amplified from P-selectin HRP²⁸ using primers incorporating 15 bp 5'
99 or 3' overlaps with Jam-C (Supp. Table 1). Jam-C-GFPout was digested with *Xba*I and *Xho*I and
100 an in-fusion reaction and subsequent transformation performed according to the
101 manufacturer's instructions (Clontech, Mountain View, CA). QuikChange site directed
102 mutagenesis of Jam-C-GFPout to generate Y267A, S281A, Y282A, K283R, K287R, Y293A and
103 T296A was performed according to the manufacturer's instructions (Agilent, Santa Clara, CA)
104 using the primers listed (Supp. Table 1). Murine Quad-K Jam-C-HRPout, Jam-C-APEX2in and
105 all the site directed mutations thereof were prepared by gene synthesis (Thermofisher,
106 Waltham, MA). The soy bean sequence was first codon optimised using GeneOptimizer
107 (Thermofisher) and incorporated into the intraluminal domain of Jam-C between the
108 transmembrane and cytoplasmic tail before subcloning into pCDNA3.1 using *Hind*III and
109 *Bam*HI sites. For lentiviral transduction WT and Quad-K Jam-C-GFPout were amplified using
110 appropriate primers (Supp. Table 1) and subcloned into pSFFV-WPRE using an infusion
111 reaction according to the manufacturer's instructions (Clontech).

112 Cell Culture and transient transfection

113 Human Umbilical Vein Endothelial Cells (HUVEC, Promocell, Heidelberg, Germany) were
114 cultured as previously described²⁹. Plasmid transfections were performed by nucleofection
115 (Nucleofector II, programme U-001, Amaxa Biosystems, Gaithersburg, MD) using 2-10 μ g DNA
116 or 250 pmol siRNA (Jam-C-AUGUAGUUAACUCCAUCUGGUUCC or CBL-1-
117 CCUCUCUCCAAGCACUGA or CBL-2-CCUGAUCUGACUGGCUUUAU).

118 Lentivirus preparation

119 To produce lentivirus, 8×10^6 HEK293T cells were seeded onto a 15 cm diameter tissue culture
120 dish in 20ml DMEM with Glutamax (Gibco) with 10% heat inactivated FBS (Gibco). Cells were
121 incubated overnight before adding 25 μ M chloroquine solution 1 hour prior to transfection.
122 Transfection complexes were prepared by diluting 18 μ g of plasmid expressing the lentiviral
123 packaging genes (pGagPol), 4 μ g plasmid expressing the VSV-G envelope (pMDVSVG), and 18
124 μ g of pSFFV-JAM-C-EGFP-WPRE in 2ml OptiMEM (Gibco). 200 μ l polyethylenimine (PEI)

125 solution (1mg/ml) was added (5:1 ratio of PEI:DNA) and immediately pulse vortexed (3 brief
126 pulses, low speed so as not to shear DNA). Complexes were incubated at room temperature
127 for 10 minutes before all volume was transferred to HEK293T cells, which were returned to
128 the incubator overnight before media was aspirated and replaced with 20 ml fresh DMEM for
129 48 hours. Virus-containing supernatant was removed and stored at 4°C, and replaced with
130 another 20 ml DMEM complete for a further 24 hours. The supernatant was taken and pooled
131 with the earlier material, syringe filtered with a 0.22 µM pore filter. 4X concentrated
132 polyethylene glycol (PEG) precipitation solution was prepared (36% PEG (6,000 Da), 1.6 M
133 NaCl, filter sterilised), and diluted to 1X concentrate in the virus containing supernatant. This
134 was stored at 4°C for 90 minutes (inverted every 30 min) before centrifugation at 1500 x g for
135 1 hour at 4°C, following which media was aspirated and the pellet resuspended in OptiMEM.
136 Aliquots were stored at -80°C until use.

137 Antibody feeding

138 HUVEC were cultured on 10 mm coverslips and inverted on pre-warmed drops of HUVEC
139 growth medium (HGM) containing 1:1000 dilution of Rabbit anti-Jam-C antibody (Supp. Table
140 2) for 15 min. Coverslips were then washed 3 times in pre-warmed PBS and transferred to a
141 drop of HGM. Coverslips were fixed at 0, 15, 30 min, 1, 2 or 4 h and immunofluorescence
142 labelled for total or cell surface antibody and the nuclei labelled with DAPI before analysis by
143 confocal microscopy. Levels of cell surface Jam-C antibody were determined using Cell Profiler
144 software^{TM30}. Nuclei and edge channels were manually Otsu thresholded and a median filter
145 was applied with an artificial diameter of 10 pixels. Objects less than 50 pixels in diameter
146 were filtered out and the object area and intensity determined.

147 Ubiquitylation assay

148 Endogenous CBL was depleted in HUVEC by two rounds of transfection with 250 pmol siRNA
149 as above. At the second round of transfection pRK5-HA-Ubiquitin-WT and WT or mutant Jam-
150 C-GFPout were included, the next day cells were lysed in RIPA buffer (150 mM NaCl, 1% NP40,
151 0.5% sodium deoxycholate, 0.1% SDS and 50mM Tris pH 8.0) supplemented with 10 mM
152 freshly prepared N-ethylmaleimide and protease inhibitors (Sigma-Aldrich). Washed GFP-
153 Trap A beads (Chromotek) were added to the lysates and incubated overnight rotating at 4°C.
154 Beads were washed and resuspended in hot laemmli buffer (2% SDS, 25% glycerol, 0.36 M β-
155 mercaptoethanol, 0.05 M Tris pH8.0) and western blotted.

156 HRP and APEX-2 proteomics

157 Typically, 4X 14 cm plates (Nunc, Roskilde, Denmark) of HUVEC were required for each
158 proteomics condition analysed. Endogenous Jam-C was depleted by two rounds of
159 transfection over a 96 h period with 250 pmol Jam-C siRNA/reaction. At the second round 10
160 µg WT, QuadK Jam-C-HRPout or APEX-2in constructs were also included. Following the second
161 round transfection cells were cultured with 7 µM freshly made heme to aid peroxidase folding
162 and in the presence or absence of 50 ng/ml TNFα and/or 100 nM Bafilomycin (Life
163 Technologies). 24 h after the second transfection, cells were fed with 500 µM biotin tyramide
164 (Iris Biotech, Marktredwitz, Germany) for 30 min at 37°C. The cells were then exposed to
165 M199 supplemented with 1 mM Hydrogen Peroxide in the presence or absence of 50 mM
166 freshly prepared ascorbate for 1 min. The biotinylation reaction was stopped by the addition
167 of stop solution (PBS, 10 mM sodium azide, 10 mM ascorbate, 5 mM Trolox). Cells were either
168 fixed for immunofluorescence analysis or lysed at 4°C in RIPA buffer supplemented with 10
169 mM sodium azide and protease inhibitors. The lysate was centrifuged at (21000 g) for 15 min
170 at 4°C and protein concentration determined (Pierce™ 660nm Protein Assay Reagent,
171 Thermo Scientific). 8.5 µg lysate was kept for western blot analysis and 1.6-1.8 mg total
172 protein was added to 250 µl washed high capacity neutravidin beads (Life Technologies) in
173 low binding tubes (Life Technologies) and rotated overnight at 4°C. The beads were washed
174 in 25 mM ammonium bicarbonate buffer, centrifuged at 21000 x g and frozen at -80°C before
175 mass spectrometry analysis.

176 Cycloheximide chase assay

177 HUVEC were transfected with WT or mutant Jam-C-GFPout, the next day cells were washed
178 and incubated with 10 µg/ml cycloheximide. Cells were lysed in RIPA buffer supplemented
179 with protease inhibitors (Sigma-Aldrich) at 0, 8 and 24 h before analysis by western blotting.

180 Mass Spectrometry

181 Proteomics experiments were performed using mass spectrometry as reported^{31, 32}. In brief,
182 Immunoprecipitated (IP) protein complex beads were digested into peptides using trypsin
183 and peptides were desalted using C18+carbon top tips (Glygen corporation, TT2MC18.96) and
184 eluted with 70% acetonitrile (ACN) with 0.1% formic acid. Dried peptides were dissolved in
185 0.1% TFA and analysed by nanoflow ultimate 3000 RSL nano instrument coupled on-line to a
186 Q Exactive plus mass spectrometer (Thermo Fisher Scientific). Gradient elution was from 3%
187 to 35% buffer B in 120 min at a flow rate 250nL/min with buffer A being used to balance the
188 mobile phase (buffer A was 0.1% formic acid in water and B was 0.1% formic acid in ACN) .

189 The mass spectrometer was controlled by Xcalibur software (version 4.0) and operated in the
190 positive mode. The spray voltage was 1.95 kV and the capillary temperature was set to 255
191 °C. The Q-Exactive plus was operated in data dependent mode with one survey MS scan
192 followed by 15 MS/MS scans. The full scans were acquired in the mass analyser at 375-
193 1500m/z with the resolution of 70 000, and the MS/MS scans were obtained with a resolution
194 of 17 500. The mass spectrometry proteomics data have been deposited to the
195 ProteomeXchange Consortium via the PRIDE partner repository with the dataset identifier
196 PXD013003. MS raw files were converted into Mascot Generic Format using Mascot Distiller
197 (version 2.5.1) and searched against the SwissProt database (release December 2015)
198 restricted to human entries using the Mascot search daemon (version 2.5.0) with an FDR of
199 ~1%. Allowed mass windows were 10 ppm and 25 mmu for parent and fragment mass to
200 charge values, respectively. Variable modifications included in searches were oxidation of
201 methionine, pyro-glu (N-term) and phosphorylation of serine, threonine and tyrosine. The
202 mascot result (DAT) files were extracted into excel files for further normalisation and
203 statistical analysis.

204 Calcium switch

205 HUVEC were washed in low calcium media (M199 with 20% dialysed FBS-SigmaAldrich and 10
206 U/ml Heparin) before addition of low calcium media with 4 mM EGTA pH 8.0. After 30 min
207 the EGTA was removed and replaced with HUVEC growth media. Cells were fixed before and
208 30 min after EGTA addition and at 15, 30, 60 and 90 min post washout. Cells were then
209 analysed by confocal microscopy labelling for Jam-C and VE-cadherin.

210 Live cell Imaging

211 Endogenous Jam-C or CBL was depleted in HUVEC by two rounds of transfection with 250
212 pmol siRNA as above. At the second round cells were transfected with WT or Quad K Jam-C-
213 GFPout and plated on borosilicate glass bottomed dishes (Greiner Bio One, Kremsmunster,
214 Austria). The following day cells were imaged in the presence or absence of 100 nM
215 Bafilomycin (Life technology) in a heat-controlled chamber at 37°C with 5% CO₂ in HUVEC
216 growth media either using 63x oil immersion objective (NA 1.3) and a Zeiss 800 microscope
217 (Zeiss, Jena, Germany) or for higher speed images using a 100x oil immersion lens (NA 1.4)
218 and a spinning disk (UltraVIEW VoX; Perkin-Elmer). During longer term timelapse (45 min)
219 images were acquired every 45 s at a resolution of 512 x 512 pixels and a step size of 0.5 µm.
220 During spinning disk acquisition images were acquired every 5 s for 10 min with a step size of

221 0.4–0.5 μm , comprising 9–14 pictures (depending on cell height) with an exposure for each
222 image at 30 ms.

223 Immunofluorescence staining

224 Fixation and staining were carried out as in Lui-Roberts et al.³³ using appropriate antibodies
225 (see Supp. Table 2). Fixed cell images were taken on a Zeiss 800 scanning confocal microscope
226 system with a 63x objective (NA 1.3) as confocal z-stacks with 0.5 μm step size. Acquisition
227 was performed using Zen Blue software with a 1024x1024 pixel resolution, 2x frame average
228 and 1x zoom.

229 Western blotting

230 Proteins were separated by SDS-PAGE, transferred to Polyvinylidene fluoride membranes
231 (PerkinElmer), and then probed with primary antibody (see Supp. Table 2) followed by the
232 appropriate HRP-conjugated secondary antibody (1:5000) (Agilent, Santa Clara, CA).

233 Scratch wound assay

234 Mock or Jam-C knock down cells were transduced with GFP, WT Jam-C-GFPout or QuadK Jam-
235 C-GFPout lentivirus. Scratch wound migration assays were performed on confluent
236 monolayers of HUVEC. Wounds were made using a pipette tip and images were captured
237 every 30 min for 16 h by time lapse microscopy using an Olympus (Shinjokum, Tokyo) IX81
238 microscope, additional images of closed scratch wounds were also acquired at 60 h.
239 Percentage wound closure was calculated using Fiji³⁴.

240 Electron microscopy

241 HUVECs were transfected with WT or Quad-K Jam-C-HRPout constructs and plated onto glass
242 coverslips. The coverslips were fixed in EM-grade 2% paraformaldehyde, 1.5% glutaraldehyde
243 (TAAB Laboratories Equipment, Ltd., Aldermaston, UK) and washed in 0.05M Tris HCl (pH7.6)
244 before incubation with 0.075% diaminobenzidine (DAB); 0.02% hydrogen peroxide for 30 min
245 in the dark. The coverslips were washed in 0.1M sodium cacodylate and secondarily fixed in
246 1% osmium tetroxide; 1.5% potassium ferricyanide and then 1% tannic acid treated. Samples
247 were then dehydrated and embedded in Epon resin. Coverslips were inverted onto pre-
248 polymerized Epon stubs and polymerized by baking at 60°C overnight. 70 nm-thin sections
249 were cut with a diatome 45° diamond knife using an ultramicrotome (UC7; Leica, Wetzlar,
250 Germany). Sections were collected on 1 × 2 mm Formvar-coated slot grids and stained with
251 Reynolds lead citrate. Samples were imaged using a transmission electron microscope (Tecnai
252 G2 Spirit; FEI, Thermofisher) and a charge-coupled device camera (SIS Morada; Olympus).

253

254 Results

255 **Jam-C is dynamically trafficked from the cell surface**

256 To characterise the amount and localisation of intracellular Jam-C present at steady state in
257 cultured endothelial cells, we carried out immunofluorescence analysis in human umbilical
258 vein endothelial cells (HUVEC) (Fig. 1A-D). In confluent monolayers, Jam-C is primarily
259 localised to the junctions although punctae of Jam-C are also present in just over half of the
260 cells (Fig. 1D). Incubating cells with the vacuolar-type H⁺-ATPase inhibitor bafilomycin
261 (100nM for 4 h) (Fig. 1C), a reagent that blocks the acidification step essential for lysosomal
262 degradation, markedly increased the number of Jam-C-positive intracellular punctae. These
263 results indicate that Jam-C is constitutively trafficked into vesicles, and at least a proportion
264 of the receptor in resting conditions is targeted for degradation in lysosomes.

265

266 We next determined the ultrastructure of intracellular Jam-C pools using electron microscopy
267 (EM). We generated a version of Jam-C fused to horse radish peroxidase (HRP) in the
268 membrane proximal region of the extracellular domain (Jam-C-HRP_{out}). Tagging of Jam-C at
269 this point has previously been shown to have no effect on ligand binding or localisation²⁷. We
270 utilised murine Jam-C for expression studies in HUVEC as this allows the depletion of
271 endogenous human Jam-C and rescue with the siRNA-resistant murine orthologue. Cells
272 expressing Jam-C-HRP_{out} were fixed and labelled with diaminobenzidine (DAB) before
273 analysis by electron microscopy. DAB labelling was present at the junctions (Fig. 1G), in small
274 endocytic clathrin-negative structures budding off from the cell surface (Fig. 1F & 1Fi),
275 endosomes (Fig. 1F) and in late endosomes/multi-vesicular bodies (MVBs) (Fig. 1H & I).

276

277 To more accurately determine the kinetics of endogenous Jam-C internalisation, we fed anti-
278 Jam-C antibody and monitored the fluorescent intensity at the junctions over a 2 h period
279 (Fig. 2A & B). This approach showed that approximately 2/3rds of surface protein are removed
280 from the junction within 2 h (Fig. 2B) indicating that Jam-C is rapidly removed from the
281 junctions at steady state.

282

283 Endothelial cell junctions are remodelled during vascular growth, angiogenesis and
284 inflammation, allowing cells to move within the monolayer and leukocytes to cross the

285 endothelial barrier. Once these processes are complete it is essential for the junctions to
286 reform to once again establish a contiguous barrier. Using immunofluorescence and confocal
287 microscopy to analyse localisation of endogenous Jam-C, we monitored the amount of
288 vesicular traffic associated with conditions that are known to disrupt endothelial barrier
289 function. We first artificially disrupted junctions by chelating calcium ions essential for
290 junctional formation³⁵; we then washed out the chelating agent (EGTA) to monitor junctional
291 reformation (Fig. 2C). An increased number of Jam-C positive vesicles was noted following the
292 addition of EGTA that then reduced following washout and formation of a confluent
293 monolayer (Fig. 2C). This indicates that vesicular trafficking of Jam-C is associated with the
294 removal of endothelial cell junctions. We next extended these studies to HUVECs treated with
295 the potent pro-inflammatory cytokines IL-1 and TNF- α . TNF- α increased the number of Jam-
296 C positive intracellular vesicles whilst IL-1 had little effect (Fig. 2D, & E), suggesting that Jam-
297 C junctional remodelling is stimulus specific.

298

299 To directly monitor the dynamics of Jam-C trafficking, we transfected HUVECs with a Jam-C-
300 GFPout construct (Fig. 2F) and observed the cells by spinning disk confocal microscopy (Fig.
301 2G, Movie 1). We noted large membranous structures forming near cellular junctions from
302 which tubular extensions were seen to emerge that subsequently detached and moved away
303 (presumably along cytoskeletal tracks), dissolving the original structure. Together, the
304 present data demonstrates that Jam-C trafficking is a rapid process, a response that is further
305 increased during junctional remodelling and following stimulation of endothelial cells with
306 certain inflammatory stimuli.

307

308 **Development of a novel HRP based proximity labelling assay for characterising the** 309 **trafficking of Jam-C**

310 The endothelial cell junction is comprised of multiple protein complexes, some of which have
311 already been demonstrated to redistribute constitutively and during leukocyte
312 transmigration³⁶⁻³⁸. To define in an unbiased manner the receptors localised with Jam-C at
313 the cell junctions and to determine which of these co-traffic with Jam-C, we developed a Jam-
314 C-HRP based proximity labelling protocol³⁹ (Fig. 3A-C). This approach uses the enzymatic
315 activity of HRP to oxidise fluid-phase fed biotin tyramide, thus generating biotin phenoxyl
316 radicals which covalently react with electron rich amino acids (such as Tyr, Trp, His and Cys)

317 on neighbouring proteins (Fig. 3B). The short-lived nature of these radicals results in a small
318 labelling radius (<20nm) and provides a proximity map of all nearby proteins (Fig. 3C). We
319 transfected HUVECs with the Jam-C-HRPout construct (Fig. 3A) and fed the cells for 30 min
320 with biotin tyramide. The proteins neighbouring Jam-C were biotinylated during a short (1
321 min) incubation with hydrogen peroxide and this reaction was then terminated using
322 molecules that scavenge free radicals. Biotinylated proteins in proximity to Jam-C HRP were
323 detected at the cell surface and within intracellular vesicles (Fig. 3D). Importantly, no
324 biotinylation was detected in the absence of the biotin tyramide or hydrogen peroxide (Supp.
325 Fig. 1A). To specifically identify intracellular stores of Jam-C, we incorporated ascorbate, a
326 membrane impermeant inhibitor of HRP, into our assay. Ascorbate blocks the proximity
327 labelling reaction at the cell surface but not in intracellular stores (Fig. 3C). This approach has
328 been previously utilised in EM studies to inhibit cell surface HRP-catalysed DAB labelling^{40, 41},
329 but to our knowledge this is the first time it has been employed for proteomics. We verified
330 that the reaction worked by immunofluorescent labelling of treated cells with fluorescently-
331 tagged streptavidin to visualise biotinylated proteins near Jam-C (Fig. 3D and Supp. Fig. 1) and
332 by western blotting using streptavidin HRP (Fig. 3E). Both methods confirmed that
333 intracellular stores of Jam-C could be visualised, but not cell surface pools. To further increase
334 the number of intracellular vesicles containing Jam-C, we also incorporated bafilomycin into
335 the assay (Fig. 3D). Following the reaction, cells were lysed and biotinylated proteins pulled
336 down with Streptavidin before performing an on-bead tryptic digest and subsequent tandem
337 mass spectrometry (MS/MS) analysis.

338

339 We detected 134 proteins that were within the vicinity of Jam-C at the cell surface and 50
340 proteins that were proximal to Jam-C after internalisation (Fig. 3F). Our mass spectrometry
341 results (Fig. 3, Supp. Table 3 – includes corrected p-value for multiple comparisons, Supp. 1B
342 &C) indicate that components of a known junctional adhesion molecule trafficking pathway,
343 the lateral border recycling compartment (LBRC) comprising PECAM-1, CD99 and Jam-A³⁶⁻³⁸
344 are all adjacent to Jam-C at the cell surface but are not co-trafficked with Jam-C. Proteins
345 classically associated with endothelial cell permeability, such as VE-Cadherin, neuropilin-1
346 and neuropilin-2, were adjacent to Jam-C at the cell surface and also co-trafficked with Jam-
347 C. Other co-trafficked receptors included plasmalemma vesicle associated protein, a protein
348 implicated in permeability, angiogenesis and leukocyte transmigration⁴², and a number of

349 integrin subunits (alpha -2,-3,-5 and beta-1). Notably VEGFR2/KDR, a receptor classically
350 associated with the neuropilins is adjacent to Jam-C at the junctions but absent from the
351 intracellular carriers, suggesting that separate trafficking of these co-receptors may be a
352 means of regulating their functions.

353

354 We further validated our MS results by immunofluorescence analysis and western blotting of
355 purified biotinylated proteins (Supp. Fig.2). Since TNF α can increase the number of Jam-C
356 positive vesicles (Fig. 2E), to determine if these are qualitatively different to those in
357 unstimulated cells (i.e. the result of an additional inflammatory pathway), or whether they
358 simply represent an upregulation in the rate of traffic, we carried out HRP proximity labelling
359 in the presence of TNF α . The co-trafficking proteins were largely the same (Supp. Fig. 3). The
360 only major difference noted was a potential reduction in the co-trafficking of Jam-C with VE-
361 Cadherin and this needs to be verified in future work. This indicates that inflammatory stimuli
362 affect the rate but not the primary route of Jam-C intracellular traffic.

363

364 **Jam-C turnover is dependent on ubiquitylation of the cytoplasmic tail**

365 To determine the importance of intracellular trafficking on the function of Jam-C we needed
366 to define the mechanism of its turnover. Trafficking of a receptor is most often governed by
367 specific signals and motifs present in the intracellular domain. The cytoplasmic domain of
368 Jam-C is relatively short (44 amino acids) and features a number of conserved potential
369 phosphorylation and ubiquitylation sites as well as a PDZ interacting domain (Fig. 4A). We
370 incorporated mutations of all these sites into our GFPout Jam-C constructs either by site
371 directed or truncation mutagenesis. When expressed in endothelial cells, all mutants
372 exhibited at least some junctional localisation (Fig. 4B). The Δ PDZ mutant exhibited a
373 noticeably different localisation in that it was expressed at higher levels and was also found
374 to be enriched in a peri-Golgi pool. To determine the effect of each mutation on Jam-C-GFP
375 turnover, we transiently transfected HUVECs with the Jam-C constructs and 16 h later added
376 cycloheximide to block new protein synthesis. We then monitored the loss of GFP-labelled
377 protein by western blot over a 24 h period (Fig. 4C and D). We observed that the K283R and
378 the Y267A mutants had slower and quicker turnover than WT Jam-C, respectively. Given that
379 increases in cell surface Jam-C levels are associated with a number of disease states including
380 atherosclerosis and rheumatoid arthritis^{19, 24}, and the K283R mutant exhibits a slower

381 turnover, we focused on the potential role of ubiquitylation in Jam-C trafficking and
382 degradation.

383

384 Jam-C has four lysine residues in its cytoplasmic tail (Fig. 5A); to completely abrogate
385 ubiquitylation, we needed to generate a mutant with all lysine residues mutated to arginine
386 (Quad-K-Jam-C). We co-transfected HUVECs with hemagglutinin (HA)-tagged ubiquitin and
387 either WT or mutant Jam-C-GFPout. Using GFP trap beads, we pulled down the tagged protein
388 and quantified levels of GFP-tagged receptor and associated HA-tagged ubiquitin (Fig. 5B).
389 The Quad-K-Jam-C was devoid of ubiquitylation unlike both the WT and EGFR protein. No
390 obvious change in Jam-C localisation was apparent with the ubiquitin mutant in fixed images
391 (Fig. 5C). However, live cell imaging of WT and Quad-K Jam-C-GFPout in the presence of
392 bafilomycin revealed marked differences in receptor trafficking (Fig. 5D & E). The WT receptor
393 gradually accrues in vesicles following bafilomycin treatment (Fig. 5D, Movie 2). These
394 structures represent the pool of late endosomes and lysosomes unable to degrade due to the
395 inhibition of V-ATPase function and therefore acidification. In contrast, Quad-K Jam-C-GFPout
396 cycles between endocytic structures and the cell surface and does not accrue in late
397 endosomal/lysosomal structures (Fig. 5E, Movie 3). This demonstrates fundamental
398 differences in receptor trafficking following blocking of Jam-C ubiquitylation. To more closely
399 examine the ultrastructure of the intracellular pools in which the Quad-K Jam-C mutant
400 localises, we incorporated the lysine mutations into the Jam-C-HRPout construct and
401 expressed it in unstimulated endothelial cells before carrying out DAB labelling and EM
402 analysis. We found clear evidence of Quad-K Jam-C-HRP on early endosomes (Fig. 5Fa) but
403 little labelling on MVBs (Fig. 5Fb & c), in contrast to WT Jam-C-HRPout (Fig. 1H & I). This data
404 is consistent with the live cell imaging experiments and indicates that the mutation of
405 intracellular lysine residues in Jam-C prevents sorting of the receptor onto the intraluminal
406 vesicles of the MVB for subsequent degradation.

407

408 **An APEX-2 proximity labelling approach to identify machinery utilised for Jam-C trafficking**

409 To determine the molecular machinery associated with the intracellular trafficking and
410 ubiquitylation of Jam-C, we used an APEX-2 proximity labelling approach. This strategy was
411 originally developed by Rhee *et al.*³⁹. To specifically identify machinery associated with

412 ubiquitylation of Jam-C, we compared WT Jam-C APEX-2 biotinylation with the Quad-K Jam-C
413 APEX-2 and monitored the proteins enriched in the former over the latter.

414

415 We incorporated a codon-optimised APEX-2 tag in the membrane proximal region of the
416 cytoplasmic tail of Jam-C in both WT and Quad-K Jam-C (Fig. 6A). This site was chosen so as
417 to minimise the potential for disrupting the C-terminal PDZ interacting domain and other
418 motifs present in the cytoplasmic tail. To ensure the WT and mutant Jam-C APEX constructs
419 did not dimerise with endogenous WT receptor, we depleted the endogenous receptor and
420 expressed siRNA-resistant constructs (Fig. 6B). We detected robust biotinylation by western
421 blot following 30 min feed with biotin tyramide and 1 min exposure to hydrogen peroxide
422 (Fig. 6C). Moreover, biotinylated proteins were detected at the junctions and on intracellular
423 vesicles following immunofluorescence labelling with streptavidin 488 (Fig. 6D). To identify
424 proteins neighbouring Jam-C-APEX, we pulled down biotinylated proteins and carried out on-
425 bead trypsin digestion and MS/MS analysis. MS analysis revealed 576 significant hits that
426 were more than 3.5 fold enriched over the mock transfected cells (Fig. 6E, F, & Supp. Table
427 4). Hits included proteins from the cell surface and intracellular pools and associated with a
428 number of cellular processes including endocytosis, recycling, fusion and ubiquitylation. We
429 detected a number of integral membrane proteins previously identified from our HRP
430 approach including VE-Cadherin. Of particular interest were a number of components
431 associated with ESCRT-0,-1 and E3 ligases such as CBL, demonstrating that at some point
432 during its trafficking, Jam-C is adjacent to machinery necessary for the ubiquitylation and the
433 maturation of endosomes to MVBs. The equivalent analysis of Quad-K Jam-C-APEX-2
434 biotinylation showed a similar profile but, notably, CBL, and components of the ESCRT
435 complex VPS28 and Vps4B were absent (Fig. 6E & G). This indicates that, when the 4 lysines
436 present in the cytoplasmic tail of Jam-C are mutated, the E3 ligase and some components of
437 the associated ESCRT machinery are not recruited, and Jam-C is therefore not sorted onto
438 intraluminal vesicles.

439

440 To confirm that CBL is required for the ubiquitylation of Jam-C we reduced its expression using
441 siRNA transfection in HUVECs (Fig. 7A). Depletion of CBL decreased the ubiquitylation of Jam-
442 C-GFPout (Fig. 7B & C) and increased the levels of receptor present in endothelial cells (Fig.
443 7B and D). The effects of CBL depletion are particularly apparent when the levels of

444 ubiquitylation are normalised to the levels of Jam-C-GFPout present (Fig. 7E). CBL knockdown
445 caused no obvious change in endogenous receptor localisation by immunofluorescence
446 analysis (Fig. 7F). However, on addition of bafilomycin, CBL depleted cells have significantly
447 fewer Jam-C-GFPout positive vesicles (Fig. 7F & G). This indicates that CBL is required for Jam-
448 C ubiquitylation, which is necessary for Jam-C sorting onto the intraluminal vesicles of late
449 endosomes.

450

451 **Ubiquitylation of Jam-C is required for cell migration**

452 Jam-C is known to mediate a number of important biological processes including
453 angiogenesis^{16, 43-46} and leukocyte transmigration⁸⁻¹². To determine how altering the ubiquitin
454 mediated-trafficking of Jam-C affects its cellular function, we performed scratch wound
455 assays. Recovery of the wound has been shown to be ameliorated in conditions of Jam-C
456 knock down⁴⁷ and increased in situations of Jam-C overexpression⁴⁸. This assay provides a
457 simple way to monitor the migration of endothelial cells, a process which is essential during
458 angiogenesis. Such changes are unlikely to be due to altered proliferation as no change in cell
459 growth has been detected following Jam-C over-expression over a 96 h period⁴⁹. We depleted
460 endogenous Jam-C and rescued with either lentiviral expressed GFP, WT Jam-C-GFPout or
461 Quad-K Jam-C-GFPout (Fig. 8A) and monitored the rate of scratch wound closure over a 16 h
462 period (Fig. 8B). The efficiency of endogenous Jam-C knockdown was similar in all conditions,
463 and the expression levels of the Jam-C constructs matched endogenous levels (Fig. 8A).
464 Knockdown of Jam-C resulted in a slower rate of scratch wound closure and this was rescued
465 by overexpression of Jam-C-GFPout (Fig. 8B & C). In contrast, Quad K Jam-C-GFPout failed to
466 rescue the phenotype (Fig. 8B & C) and 60 h post scratch the wound remained open (Fig. 8D).

467

468 Finally, we used live cell imaging to directly analyse the trafficking of Jam-C in migrating cells
469 (Fig. 9A, Movie 4). We noted large Jam-C-GFPout positive vesicles forming at junctional sites
470 on either side of the cell's leading edge; no such vesicle traffic was apparent at the very front
471 of migrating cells. This indicates that junctional disassembly is a crucial aspect of cell migration
472 and a proportion of this internalised Jam-C needs to be degraded by a ubiquitin-mediated
473 lysosomal pathway to allow normal cell migration (Fig. 8). Together, the results demonstrate
474 dynamic Jam-C trafficking and ubiquitylation are essential responses for endothelial cell
475 migration.

476 Discussion

477 Prior to this study many aspects of the molecular control of Jam-C function were unclear. As
478 was the relationship, in terms of regulation and function, with its orthologue Jam-A and other
479 components of the junctional machinery. Our presented work addresses many of these issues
480 and opens further avenues of research to determine how intracellular trafficking controls
481 Jam-C's important physiological and pathological roles.

482

483 Our proximity labelling proteomics approach allowed a bulk analysis of the receptors
484 trafficked alongside Jam-C. With this approach we discovered that Jam-C traffics with VE-
485 Cadherin, NRP-1 and -2 as well as some integrin subunits, but is not present in the same pool
486 as its orthologue Jam-A or any of the other component of the LBRC. This co-trafficking is likely
487 to represent receptors associated with a similar function being moved on mass. Receptors
488 present in the LBRC are thought to provide a reticular pool of unligated receptors necessary
489 for leukocyte movement whilst by contrast we hypothesise trafficking of Jam-C and its
490 counterparts allow precise control of cell migration and the passage of molecules and cells by
491 disassembling and reforming the junction. In agreement with this we see increased trafficking
492 of Jam-C associated with artificial disruption of the junctions by calcium chelation and
493 following exposure to an inflammatory stimulus (TNF α). Another cytokine, IL-1 had little
494 effect on trafficking and this difference likely reflects the ability of TNF α signalling to
495 additionally stimulate an endothelial permeability response⁵⁰. *In vivo* TNF α signalling is known
496 to be important during ischemia reperfusion injury⁵¹ one of the first occasions in which
497 vesicular pools of Jam-C were noted¹⁰.

498

499 Although there is no direct co-dependence for traffic, it remains possible that Jam-C may
500 share some as yet unknown trafficking machinery with its neighbours and be internalised at
501 the same time from the cell surface. However, some of the receptors present in the same co-
502 trafficked pool have been reported to be internalised by different clathrin dependent and
503 independent routes⁵²⁻⁵⁶. An alternative explanation is that the shared pool could represent a
504 fusion of early endosomes from diverse endocytic routes to form a late endosomal pool
505 downstream. There is therefore scope for co-trafficked receptors interacting with each other
506 and therefore modifying function although this remains to be investigated.

507

508 A key finding of the study is that we show for the first time that Jam-C is ubiquitylated and
509 that this modification represents a key step in Jam-C receptor trafficking. Our APEX-2
510 proximity labelling approach allowed us to identify CBL as the E-3 ligase responsible for
511 ubiquitylating Jam-C on up to 4 different residues in the cytoplasmic domain, with the number
512 and the pattern of bands suggesting polyubiquitylation. This modification is necessary for the
513 efficient sorting of Jam-C onto intraluminal vesicles of the MVB. The trafficking phenotype on
514 CBL depletion was less striking than that of the Quad-K Jam-C mutant, and so likely represents
515 either an incomplete block of the ubiquitylation pathway or compensation by another E3
516 ligase. Ubiquitylation is a means of controlling turnover of claudin -1, -2, -4, -5, -8 and -16⁵⁷
517 however the only Jam family member previously shown to be ubiquitylated is Jam-B on Sertoli
518 cells, the site of ubiquitylation, the E3 ligase involved, and the effect on receptor trafficking
519 has yet to be determined⁵⁸. A further means to regulate Jam-C trafficking and function is likely
520 to be the removal of ubiquitin. There are thought to be more than 100 potential
521 deubiquitinating enzymes (DUB) in mammalian cells⁵⁷ and we identified 6 potential Jam-C
522 localised DUBs in our APEX-2 screen USP-5, -7, -10, -15, -47 and USPY. Notably, these proteins
523 were adjacent to Jam-C irrespective of whether we utilised the WT or the Quad-K mutant and
524 therefore could potentially represent nearby bystander proteins rather than bona fide
525 interactors. We have yet to verify if these proteins are important for Jam-C traffic although
526 interestingly USP-47 has been shown to regulate E-cadherin deubiquitylation at junctions⁵⁹.

527

528 Our results show that targeted removal and degradation of Jam-C from junctions is required
529 for endothelial cell migration. As endothelial cells migrate to fill a gap in the monolayer,
530 endocytic disassembly of the junction occurs either side of the cells leading edge. As Jam-C
531 enters endosomes it becomes ubiquitylated and is directed for degradation by the lysosomes.
532 A failure to ubiquitylate has no effect on internalisation but results in premature recycling of
533 Jam-C back to the cell surface. We present two potential models (which are not mutually
534 exclusive) of how inhibition of degradation of Jam-C slows migration (Fig. 9B). Firstly, the
535 change in receptor recycling might prematurely increase the strength of homo and
536 heterotypic junctional interactions with neighbouring cells preventing cell movement.
537 Secondly, targeting receptor for degradation might be required to disrupt cell surface protein-
538 protein interactions or terminate signalling events. Such signalling could potentially occur via
539 interactions with the polarity proteins Par3⁶⁰ and Par6⁶¹. Notably Par3/Jam-C interactions are

540 required for neuronal cell migration from the germinal zone⁶² and signalling via Par3 and
541 Cdc42 is required for lumen formation during 3D endothelial tubulogenesis⁶³.

542

543 The trafficking and degradation of Jam-C is likely important for the other ascribed roles of
544 Jam-C, particularly during leukocyte transmigration and permeability as they both rely on the
545 disassembly and reassembly of junctions. Controlling the trafficking of Jam-C and its co-
546 trafficked counterparts could potentially provide novel ways of limiting disease states,
547 particularly those associated with increased levels of cell surface Jam-C, such as
548 atherosclerosis and arthritis.

549

550 Acknowledgments

551 Funding

552 T.D. Nightingale, C. Schultz and K. Kostelnik were funded by an MRC project grant
553 MR/M019179/1. The research leading to these results has also received funding from the
554 People Programme (Marie Curie Actions) of the European Union's Seventh Framework
555 Programme (FP7/2007-2013) under REA grant agreement n° 608765. A. Barker was funded
556 by QMUL. S. Nourshargh was funded by a Wellcome Trust investigator award 098291/Z/12/Z.
557 M. Aurrand Lions was funded by Canceropôle PACA (Valo-Paca 2016) and French National
558 Institute of Cancer (Inca, PRT-K16, #2017-24). P. Cutillas and V. Rajeeve were funded by BBSRC
559 (BB/M006174/1) and the Barts and The London Charity (297/2249). I.J. White was funded by
560 an MRC LMCB core grant award MC_U12266B.

561

562 References

- 563 1. Zihni, C., Mills, C., Matter, K. & Balda, M.S. Tight junctions: from simple barriers to
564 multifunctional molecular gates. *Nat Rev Mol Cell Biol* **17**, 564-80 (2016).
- 565 2. Nourshargh, S. & Alon, R. Leukocyte migration into inflamed tissues. *Immunity* **41**,
566 694-707 (2014).
- 567 3. Ramasamy, S.K., Kusumbe, A.P. & Adams, R.H. Regulation of tissue morphogenesis by
568 endothelial cell-derived signals. *Trends Cell Biol* **25**, 148-57 (2015).
- 569 4. Godo, S. & Shimokawa, H. Endothelial Functions. *Arterioscler Thromb Vasc Biol* **37**,
570 e108-e114 (2017).
- 571 5. Malinova, T.S. & Huvneers, S. Sensing of Cytoskeletal Forces by Asymmetric
572 Adherens Junctions. *Trends Cell Biol* **28**, 328-341 (2018).
- 573 6. Ebnet, K. Junctional Adhesion Molecules (JAMs): Cell Adhesion Receptors With
574 Pleiotropic Functions in Cell Physiology and Development. *Physiol Rev* **97**, 1529-1554
575 (2017).

- 576 7. Reglero-Real, N., Colom, B., Bodkin, J.V. & Nourshargh, S. Endothelial Cell Junctional
577 Adhesion Molecules: Role and Regulation of Expression in Inflammation. *Arterioscler*
578 *Thromb Vasc Biol* **36**, 2048-2057 (2016).
- 579 8. Bradfield, P.F. et al. JAM-C regulates unidirectional monocyte transendothelial
580 migration in inflammation. *Blood* **110**, 2545-55 (2007).
- 581 9. Chavakis, T. et al. The junctional adhesion molecule-C promotes neutrophil
582 transendothelial migration in vitro and in vivo. *J Biol Chem* **279**, 55602-8 (2004).
- 583 10. Scheiermann, C. et al. Junctional adhesion molecule-C mediates leukocyte infiltration
584 in response to ischemia reperfusion injury. *Arterioscler Thromb Vasc Biol* **29**, 1509-15
585 (2009).
- 586 11. Woodfin, A. et al. The junctional adhesion molecule JAM-C regulates polarized
587 transendothelial migration of neutrophils in vivo. *Nat Immunol* **12**, 761-9 (2011).
- 588 12. Zen, K. et al. JAM-C is a component of desmosomes and a ligand for CD11b/CD18-
589 mediated neutrophil transepithelial migration. *Mol Biol Cell* **15**, 3926-37 (2004).
- 590 13. Li, X. et al. JAM-C induces endothelial cell permeability through its association and
591 regulation of β_3 integrins. *Arterioscler Thromb Vasc Biol* **29**, 1200-6 (2009).
- 592 14. Orlova, V.V. & Chavakis, T. Regulation of vascular endothelial permeability by
593 junctional adhesion molecules (JAM). *Thromb Haemost* **98**, 327-32 (2007).
- 594 15. Orlova, V.V., Economopoulou, M., Lupu, F., Santoso, S. & Chavakis, T. Junctional
595 adhesion molecule-C regulates vascular endothelial permeability by modulating VE-
596 cadherin-mediated cell-cell contacts. *J Exp Med* **203**, 2703-14 (2006).
- 597 16. Rabquer, B.J. et al. Junctional adhesion molecule-C is a soluble mediator of
598 angiogenesis. *J Immunol* **185**, 1777-85 (2010).
- 599 17. Colom, B. et al. Leukotriene B₄-Neutrophil Elastase Axis Drives Neutrophil Reverse
600 Transendothelial Cell Migration In Vivo. *Immunity* **42**, 1075-86 (2015).
- 601 18. Wu, D. et al. Reverse-migrated neutrophils regulated by JAM-C are involved in acute
602 pancreatitis-associated lung injury. *Sci Rep* **6**, 20545 (2016).
- 603 19. Palmer, G. et al. Expression and function of junctional adhesion molecule-C in human
604 and experimental arthritis. *Arthritis Res Ther* **9**, R65 (2007).
- 605 20. Vonlaufen, A. et al. The role of junctional adhesion molecule C (JAM-C) in acute
606 pancreatitis. *J Pathol* **209**, 540-8 (2006).
- 607 21. Aurrand-Lions, M. et al. Junctional adhesion molecule-C regulates the early influx of
608 leukocytes into tissues during inflammation. *J Immunol* **174**, 6406-15 (2005).
- 609 22. Imhof, B.A. et al. Pulmonary dysfunction and impaired granulocyte homeostasis result
610 in poor survival of Jam-C-deficient mice. *J Pathol* **212**, 198-208 (2007).
- 611 23. Bradfield, P.F. et al. Divergent JAM-C Expression Accelerates Monocyte-Derived Cell
612 Exit from Atherosclerotic Plaques. *PLoS One* **11**, e0159679 (2016).
- 613 24. Keiper, T. et al. The role of junctional adhesion molecule-C (JAM-C) in oxidized LDL-
614 mediated leukocyte recruitment. *FASEB J* **19**, 2078-80 (2005).
- 615 25. Shagdarsuren, E. et al. Importance of junctional adhesion molecule-C for neointimal
616 hyperplasia and monocyte recruitment in atherosclerosis-prone mice-brief report.
617 *Arterioscler Thromb Vasc Biol* **29**, 1161-3 (2009).
- 618 26. Sircar, M. et al. Neutrophil transmigration under shear flow conditions in vitro is
619 junctional adhesion molecule-C independent. *J Immunol* **178**, 5879-87 (2007).
- 620 27. Lamagna, C. et al. Dual interaction of JAM-C with JAM-B and $\alpha(M)\beta_2$ integrin:
621 function in junctional complexes and leukocyte adhesion. *Mol Biol Cell* **16**, 4992-5003
622 (2005).

- 623 28. Norcott, J.P., Solari, R. & Cutler, D.F. Targeting of P-selectin to two regulated secretory
624 organelles in PC12 cells. *J Cell Biol* **134**, 1229-40 (1996).
- 625 29. Michaux, G. et al. The physiological function of von Willebrand's factor depends on its
626 tubular storage in endothelial Weibel-Palade bodies. *Dev Cell* **10**, 223-32 (2006).
- 627 30. Carpenter, A.E. et al. CellProfiler: image analysis software for identifying and
628 quantifying cell phenotypes. *Genome Biol* **7**, R100 (2006).
- 629 31. Casado, P. et al. Kinase-substrate enrichment analysis provides insights into the
630 heterogeneity of signaling pathway activation in leukemia cells. *Sci Signal* **6**, rs6
631 (2013).
- 632 32. Rajeeve, V., Vendrell, I., Wilkes, E., Torbett, N. & Cutillas, P.R. Cross-species
633 proteomics reveals specific modulation of signaling in cancer and stromal cells by
634 phosphoinositide 3-kinase (PI3K) inhibitors. *Mol Cell Proteomics* **13**, 1457-70 (2014).
- 635 33. Lui-Roberts, W.W., Collinson, L.M., Hewlett, L.J., Michaux, G. & Cutler, D.F. An AP-
636 1/clathrin coat plays a novel and essential role in forming the Weibel-Palade bodies of
637 endothelial cells. *J Cell Biol* **170**, 627-36 (2005).
- 638 34. Schindelin, J. et al. Fiji: an open-source platform for biological-image analysis. *Nat*
639 *Methods* **9**, 676-82 (2012).
- 640 35. Hong, S., Troyanovsky, R.B. & Troyanovsky, S.M. Cadherin exits the junction by
641 switching its adhesive bond. *J Cell Biol* **192**, 1073-83 (2011).
- 642 36. Mamdouh, Z., Kreitzer, G.E. & Muller, W.A. Leukocyte transmigration requires kinesin-
643 mediated microtubule-dependent membrane trafficking from the lateral border
644 recycling compartment. *J Exp Med* **205**, 951-66 (2008).
- 645 37. Mamdouh, Z., Mikhailov, A. & Muller, W.A. Transcellular migration of leukocytes is
646 mediated by the endothelial lateral border recycling compartment. *J Exp Med* **206**,
647 2795-808 (2009).
- 648 38. Sullivan, D.P. & Muller, W.A. Neutrophil and monocyte recruitment by PECAM, CD99,
649 and other molecules via the LBRC. *Semin Immunopathol* (2013).
- 650 39. Rhee, H.W. et al. Proteomic mapping of mitochondria in living cells via spatially
651 restricted enzymatic tagging. *Science* **339**, 1328-1331 (2013).
- 652 40. Hopkins, C., Gibson, A., Stinchcombe, J. & Futter, C. Chimeric molecules employing
653 horseradish peroxidase as reporter enzyme for protein localization in the electron
654 microscope. *Methods Enzymol* **327**, 35-45 (2000).
- 655 41. Stoorvogel, W., Oorschot, V. & Geuze, H.J. A novel class of clathrin-coated vesicles
656 budding from endosomes. *J Cell Biol* **132**, 21-33 (1996).
- 657 42. Keuschnigg, J. et al. The prototype endothelial marker PAL-E is a leukocyte trafficking
658 molecule. *Blood* **114**, 478-84 (2009).
- 659 43. Economopoulou, M. et al. Endothelial-specific deficiency of Junctional Adhesion
660 Molecule-C promotes vessel normalisation in proliferative retinopathy. *Thromb*
661 *Haemost* **114**, 1241-9 (2015).
- 662 44. Hao, S. et al. JAM-C promotes lymphangiogenesis and nodal metastasis in non-small
663 cell lung cancer. *Tumour Biol* **35**, 5675-87 (2014).
- 664 45. Hou, X. et al. Targeting of junctional adhesion molecule-C inhibits experimental
665 choroidal neovascularization. *Invest Ophthalmol Vis Sci* **53**, 1584-91 (2012).
- 666 46. Lamagna, C., Hodivala-Dilke, K.M., Imhof, B.A. & Aurrand-Lions, M. Antibody against
667 junctional adhesion molecule-C inhibits angiogenesis and tumor growth. *Cancer Res*
668 **65**, 5703-10 (2005).

- 669 47. Hao, S. et al. JAM-C promotes lymphangiogenesis and nodal metastasis in non-small
670 cell lung cancer. *Tumour Biol* (2014).
- 671 48. Mandicourt, G., Iden, S., Ebnet, K., Aurrand-Lions, M. & Imhof, B.A. JAM-C regulates
672 tight junctions and integrin-mediated cell adhesion and migration. *J Biol Chem* **282**,
673 1830-7 (2007).
- 674 49. Fuse, C., Ishida, Y., Hikita, T., Asai, T. & Oku, N. Junctional adhesion molecule-C
675 promotes metastatic potential of HT1080 human fibrosarcoma. *J Biol Chem* **282**, 8276-
676 83 (2007).
- 677 50. Vandenbroucke, E., Mehta, D., Minshall, R. & Malik, A.B. Regulation of endothelial
678 junctional permeability. *Ann N Y Acad Sci* **1123**, 134-45 (2008).
- 679 51. Kalogeris, T., Baines, C.P., Krenz, M. & Korthuis, R.J. Cell biology of
680 ischemia/reperfusion injury. *Int Rev Cell Mol Biol* **298**, 229-317 (2012).
- 681 52. Lakshminarayan, R. et al. Galectin-3 drives glycosphingolipid-dependent biogenesis of
682 clathrin-independent carriers. *Nat Cell Biol* **16**, 595-606 (2014).
- 683 53. Orsenigo, F. et al. Phosphorylation of VE-cadherin is modulated by haemodynamic
684 forces and contributes to the regulation of vascular permeability in vivo. *Nat Commun*
685 **3**, 1208 (2012).
- 686 54. Salikhova, A. et al. Vascular endothelial growth factor and semaphorin induce
687 neuropilin-1 endocytosis via separate pathways. *Circ Res* **103**, e71-9 (2008).
- 688 55. Wessel, F. et al. Leukocyte extravasation and vascular permeability are each
689 controlled in vivo by different tyrosine residues of VE-cadherin. *Nat Immunol* **15**, 223-
690 30 (2014).
- 691 56. Xiao, K. et al. p120-Catenin regulates clathrin-dependent endocytosis of VE-cadherin.
692 *Mol Biol Cell* **16**, 5141-51 (2005).
- 693 57. Cai, J., Culley, M.K., Zhao, Y. & Zhao, J. The role of ubiquitination and deubiquitination
694 in the regulation of cell junctions. *Protein Cell* **9**, 754-769 (2018).
- 695 58. Zhang, X. & Lui, W.Y. Transforming growth factor-beta3 regulates cell junction
696 restructuring via MAPK-mediated mRNA destabilization and Smad-dependent protein
697 degradation of junctional adhesion molecule B (JAM-B). *Biochim Biophys Acta* **1849**,
698 601-11 (2015).
- 699 59. Sako-Kubota, K., Tanaka, N., Nagae, S., Meng, W. & Takeichi, M. Minus end-directed
700 motor KIFC3 suppresses E-cadherin degradation by recruiting USP47 to adherens
701 junctions. *Mol Biol Cell* **25**, 3851-60 (2014).
- 702 60. Ebnet, K. et al. The junctional adhesion molecule (JAM) family members JAM-2 and
703 JAM-3 associate with the cell polarity protein PAR-3: a possible role for JAMs in
704 endothelial cell polarity. *J Cell Sci* **116**, 3879-91 (2003).
- 705 61. Gliki, G., Ebnet, K., Aurrand-Lions, M., Imhof, B.A. & Adams, R.H. Spermatid
706 differentiation requires the assembly of a cell polarity complex downstream of
707 junctional adhesion molecule-C. *Nature* **431**, 320-4 (2004).
- 708 62. Famulski, J.K. et al. Siah regulation of Pard3A controls neuronal cell adhesion during
709 germinal zone exit. *Science* **330**, 1834-8 (2010).
- 710 63. Sacharidou, A. et al. Endothelial lumen signaling complexes control 3D matrix-specific
711 tubulogenesis through interdependent Cdc42- and MT1-MMP-mediated events.
712 *Blood* **115**, 5259-69 (2010).
- 713
714

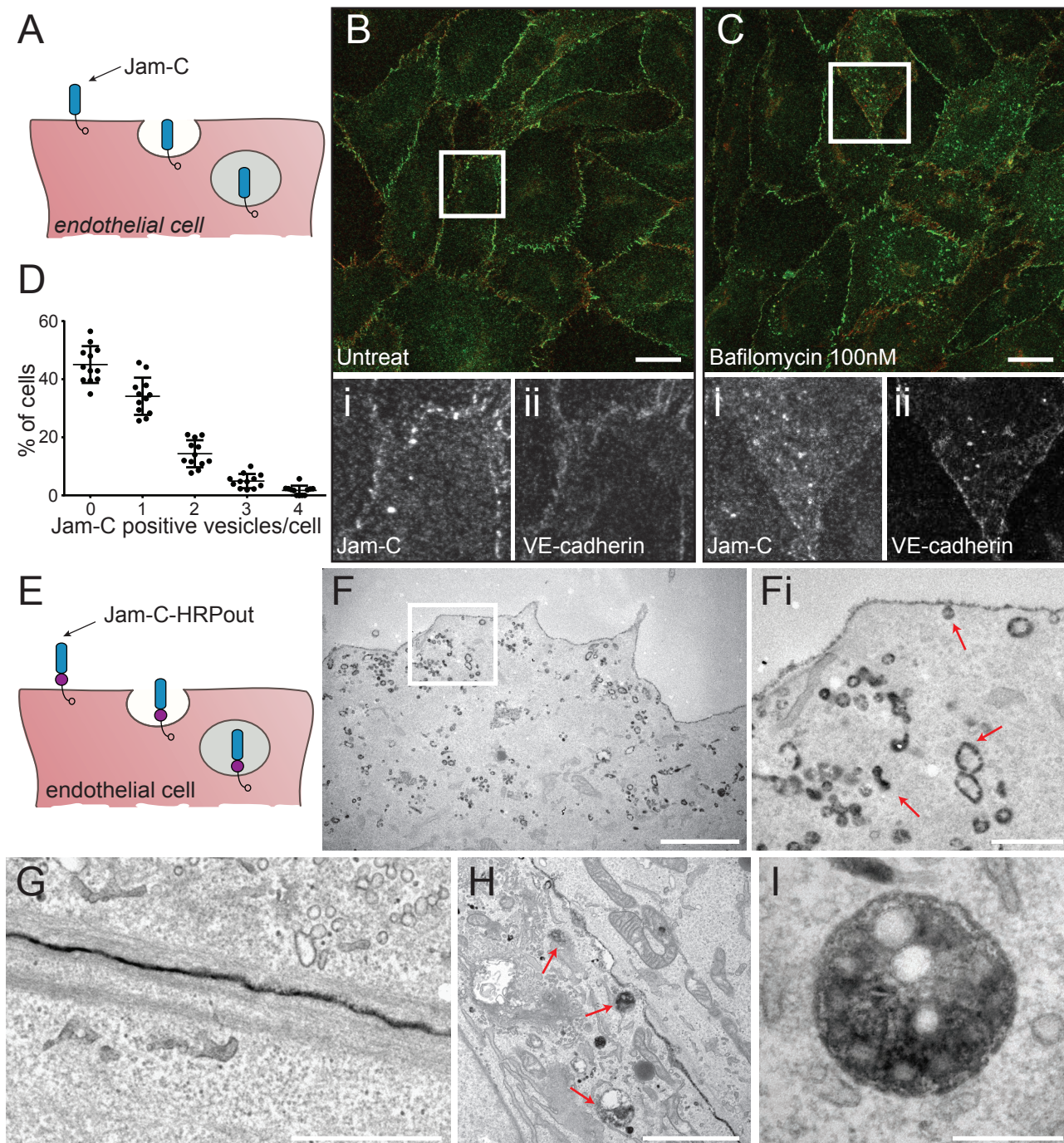


Figure 1 Jam-C is constitutively trafficked from endothelial cell junctions.

(A) Schematic of the endocytosis of endogenous Jam-C from the endothelial cell surface showing the extracellular immunoglobulin domains (blue) and the intracellular PDZ interacting domain (clear circle). (B) Untreated or (C) 100nM bafilomycin treated HUVEC were fixed and co-stained for Jam-C (green) and VE-Cadherin (red). Boxed regions are shown magnified below in greyscale (i) Jam-C (ii) VE-Cadherin. Scale bar 20µm. (D) Quantification of the % of untreated cells with a number of Jam-C positive vesicles (551 cells from n=3 experiments, error bars represent SEM). (E) Schematic of the endocytosis of Jam-C-HRPout from the endothelial cell surface showing the extracellular immunoglobulin domains (blue), the HRP tag (purple circle) and the intracellular PDZ interacting domain (clear circle). (F-I) HUVEC were transiently transfected with Jam-C-HRPout, fixed and incubated with diaminobenzidine (DAB) and hydrogen peroxide for 30min. Cells were then secondarily fixed and 70nm sections prepared and imaged by transmission electron microscopy. Precipitated DAB can be clearly seen on (F) endocytic structures and early endosomes, (Fi) shows boxed area magnified, red arrows highlight endocytic structures and endosomes, (G) junctions, (H and I) multi-vesicular bodies (red arrows). Scale bars (F) 2 µm (Fi) 500 nm (G) 1 µm (H) 2 µm (I) 200 nm.

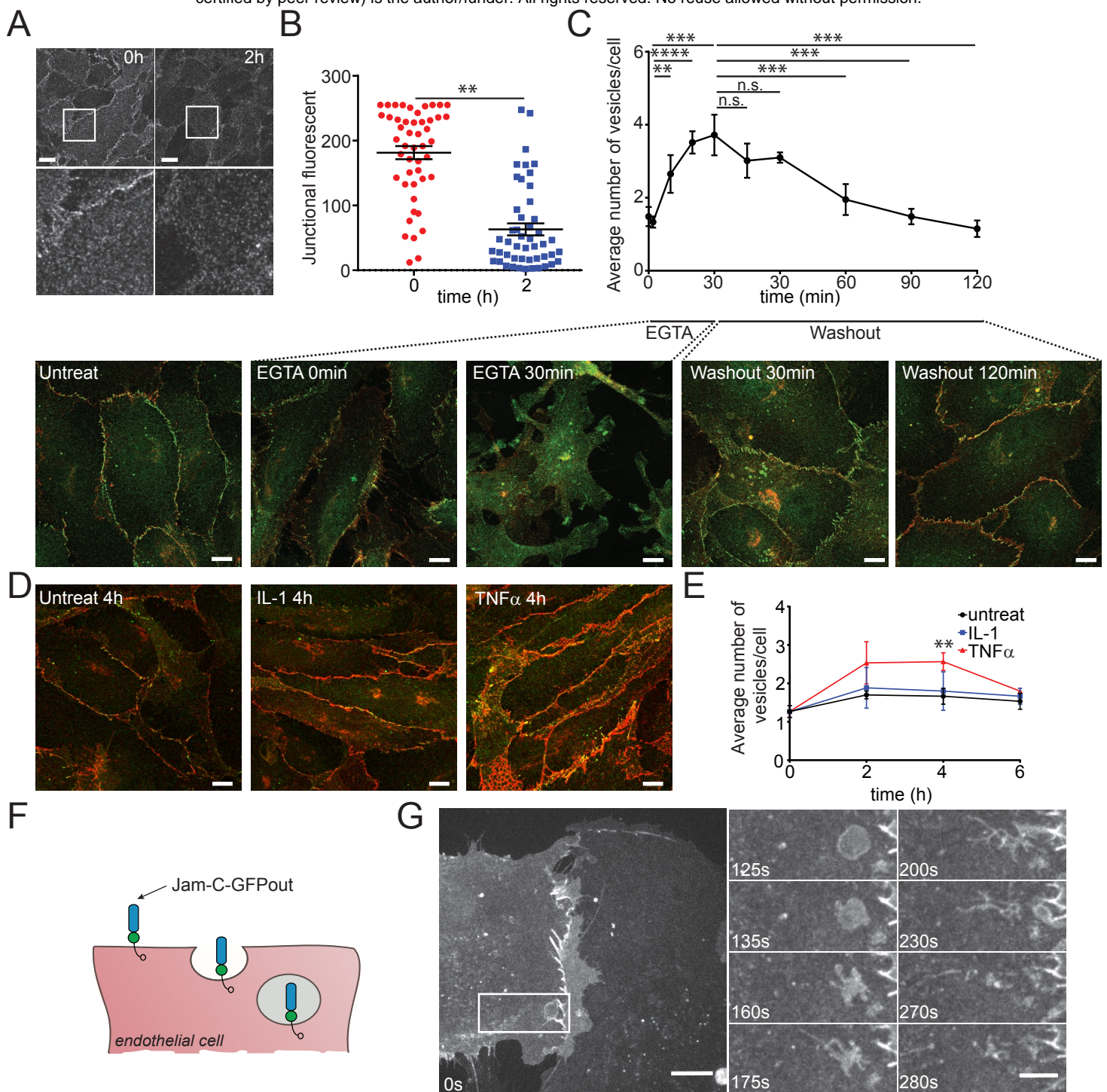


Figure. 2 Jam-C is turned over dynamically at the endothelial junction and the rate of internalisation is increased during junctional disassembly and inflammation.

(A) HUVEC were fed with Jam-C antibody, excess antibody was removed and the cells were incubated at 37°C before being fixed at 0 and 2 h and imaged by confocal microscopy. Scale bar 20 μ m, boxed regions are shown at higher magnification. (B) The difference in junctional intensity is quantified between 0 and 2 h (n=4 experiments, error bars represent SEM, $^{**}P \leq 0.01$; t-test). (C) HUVEC were treated with 4 mM EGTA in calcium free low serum media for 30 min before washing and incubation at 37°C with conventional media. Cells were fixed before and during the time course of wash out and recovery and stained for Jam-C (green) and VE-Cadherin (red). Images were acquired by confocal microscopy and the number of Jam-C positive vesicles at each time point determined. Scale bar 10 μ m (5 fields of view/experiment, n=3 experiments, error bars represent SD, $^{**}P \leq 0.01$, $^{***}P \leq 0.001$, $^{****}P \leq 0.0001$; t test). (D) HUVEC were either left untreated or incubated with 10 ng/ml IL-1 or 50 ng/ml TNF α for 4h at 37°C. Cells were then fixed and stained for Jam-C (green) and VE-Cadherin (red). Images were acquired by confocal microscopy and (E) the number of Jam-C positive vesicles at each time point determined. Scale bar 10 μ m (150 cells from n=3 experiments, error bars represent SD, $^{**}P \leq 0.01$; t test). (F) Schematic of the endocytosis of Jam-C-GFPout from the endothelial cell surface showing the extracellular immunoglobulin domains (blue), the GFP tag (green circle) and the intracellular PDZ interacting domain (clear circle). (G) HUVEC were nucleofected with WT JAM-C-GFPout and imaged with a spinning-disk confocal microscope. Time indicates total time in media and the boxed region at 0 s is shown magnified at later time points. Jam-C exists in vesicles, at the cell surface and at the cell junctions. Large vesicles can be seen that tubulate and migrate away from the junctional region. Scale bar: 0s, 20 μ m; inset, 10 μ m.

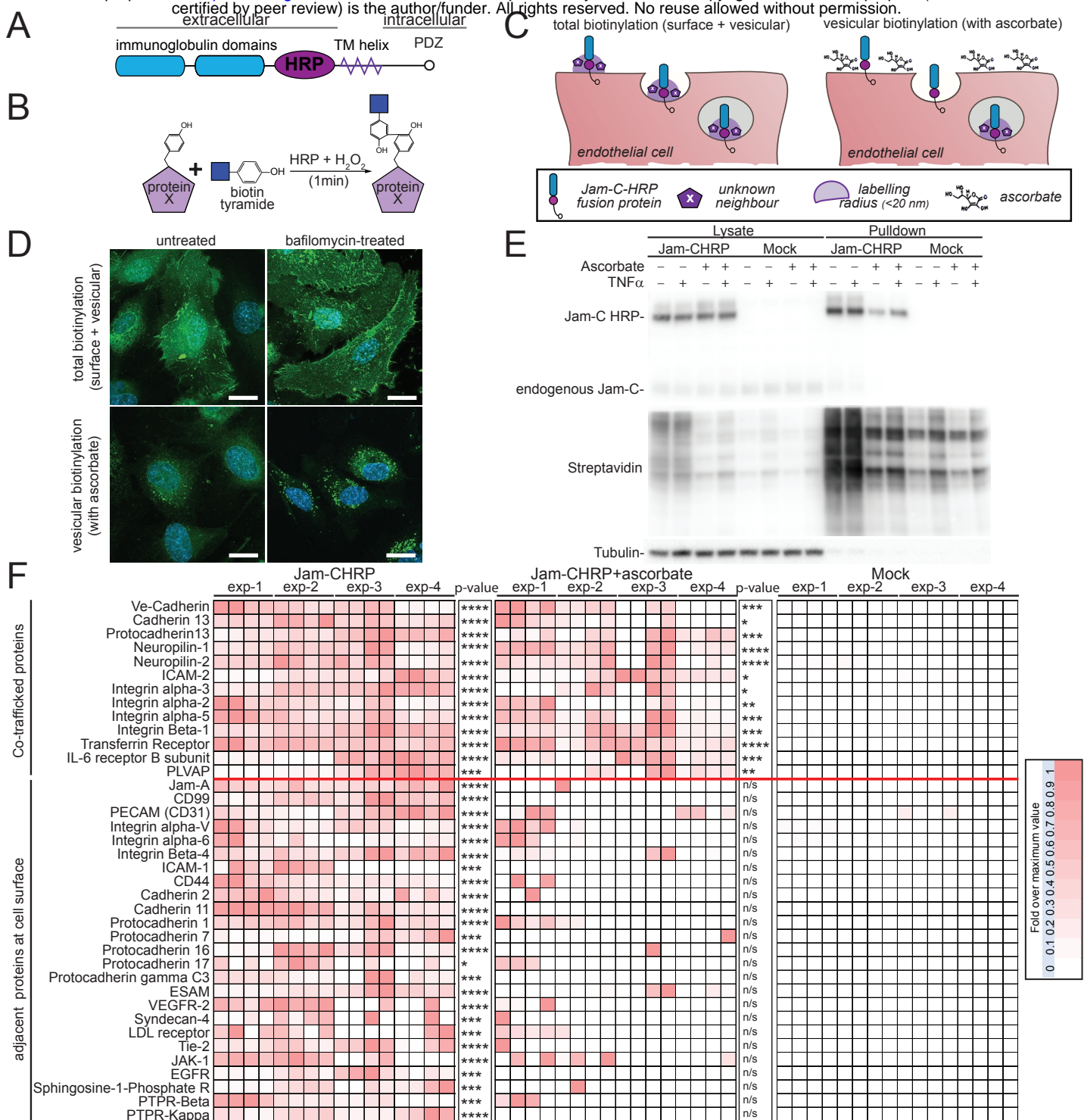


Figure 3 An HRP based proximity labelling approach reveals Jam-C co-traffics with NRP-1, -2 and VE-Cadherin but not with components of the lateral border recycling compartment.

(A) Schematic of the domain structure of the Jam-C HRP construct. (B) In the presence of biotin tyramide and hydrogen peroxide the HRP tag leads to the biotinylation of any proteins within 20 nm (labelled with an X) on Tyrosine, Tryptophan, Cysteine or Histidine residues. (C) Endothelial cells expressing Jam-C-HRP_{out} are fed with biotin tyramide and then hydrogen peroxide is added for 1 min. Proteins within 20 nm radius of Jam-C-HRP are labelled with biotin (shown in light purple). Addition of the membrane impermeant HRP inhibitor ascorbate blocks the biotinylation reaction at the cell surface but not inside the cell. (D-F) HUVEC were transfected with Jam-C-HRP_{out} and incubated in the presence or absence of bafilomycin A1 (100 nM) for 4 h to block lysosomal degradation. Cells were fed biotin tyramide for 30 min and then exposed to hydrogen peroxide for 1 min in the presence or absence of 50 mM ascorbate. (D) The cells were then fixed and labelled for streptavidin (green) and DAPI (blue) and images acquired by confocal microscopy. Scale bar 20 μ m or (E-F) The reaction was then quenched and the cells lysed. Biotinylated proteins were pulled down using neutravidin beads and lysate and pulldown samples were analysed by (E) SDS PAGE and western blot, for the presence of Jam-C, tubulin and biotinylated proteins or (F) following an on bead tryptic digest mass spectrometry. A heat map of 4 independent mass spectrometry data sets is shown with white none and dark red a high signal. Individual experiments were carried out in duplicate with each mass spectrometry run being repeated twice (to give a total of 4 analyses/experiment). P values are given across all 4 experiments (* $P \leq 0.05$, ** $P \leq 0.01$, *** $P \leq 0.001$, **** $P \leq 0.0001$ *t*-test). The + TNF experiment is shown in Supp. Fig. 3. Co-trafficked proteins appear in both +/- ascorbate conditions whilst proteins adjacent to Jam-C solely at the cell surface are only present in the - ascorbate condition.

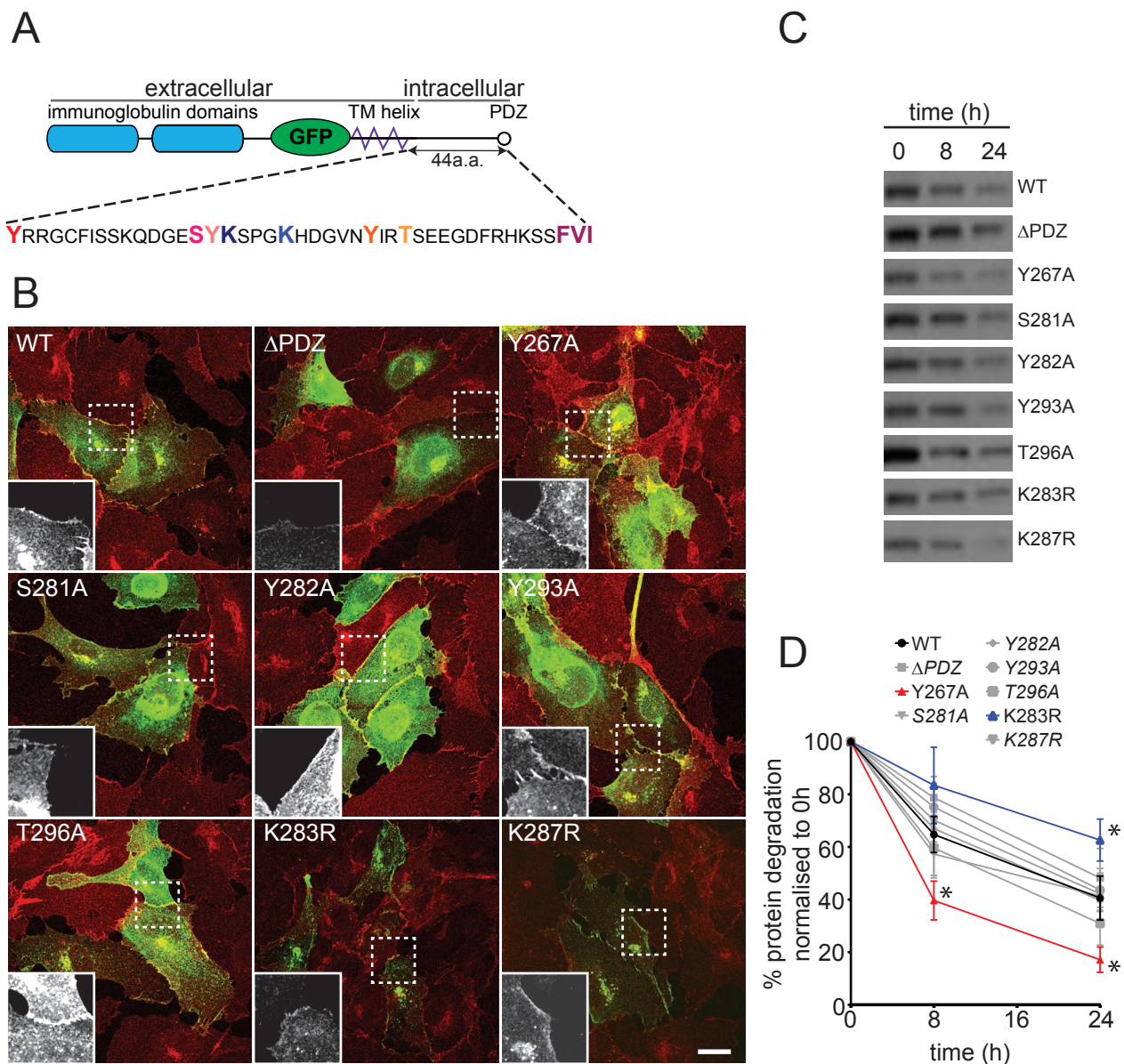


Figure 4 A lysine residue in the cytoplasmic tail of Jam-C is required for its timely degradation.

(A) A schematic representation of the Jam-C-GFPout construct showing the residues in the cytoplasmic tail that were mutated by site directed mutagenesis. (B) HUVEC cells were transfected with WT or mutant Jam-C-GFPout constructs, fixed and stained for VE-Cadherin (red). The boxed area is magnified (bottom left of each panel) to show the Jam-C-GFP signal. All Jam-C mutants exhibit at least some junctional staining. The Δ PDZ construct exhibited the most marked change in localisation existing additionally in a peri-Golgi region and expressing at higher levels. Scale bars 20 μ m. (C & D) HUVEC were transfected with WT or mutated Jam-C-GFPout constructs and treated with 10 μ g/ml cycloheximide. (C) The rate of protein degradation was determined by SDS PAGE and western blot over a 24 h period, a representative anti-GFP blot is shown. (D) Quantification of western blots normalised to the 0 h protein levels, data from n=7 experiments, error bars represent SEM (* $P \leq 0.05$; two-way ANOVA).

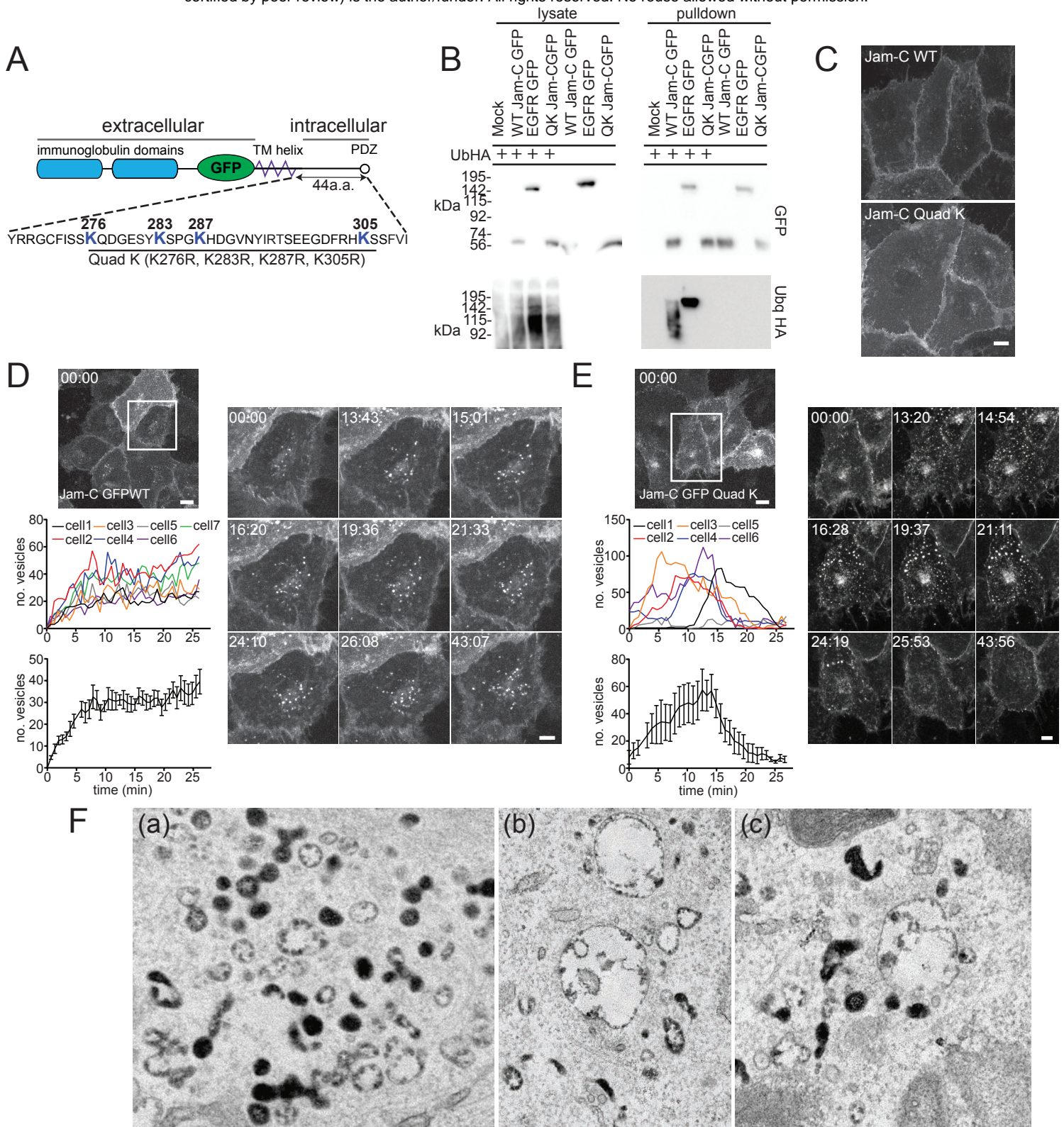


Figure 5 Jam-C is ubiquitylated and this governs its targeting to multi-vesicular bodies.

(A) A schematic representation of the Jam-C EGFP Out construct showing all the lysine residues in the cytoplasmic tail that can be potentially modified by ubiquitylation and the Jam-C mutant generated. (B) HUVEC were transfected with WT or Quad K Jam-C-GFPout and Ubiquitin HA. Cells were lysed and GFP tagged proteins were pulled down using GFP trap agarose beads. Lysate and pulldown proteins were analysed by SDS PAGE and western blot for the presence of GFP and HA tagged proteins. WT but not Quad-K Jam-C is modified with ubiquitin. (C) HUVEC were transfected with WT or Quad-K mutant Jam-C-GFPout and then fixed before imaging by confocal microscopy. Scale bar 20 μ m. (D & E) HUVEC were transfected with (D) WT or (E) Quad-K Jam-C-EGFPout and 100 nM Bafilomycin was added (at t=0 min) before imaging by timelapse confocal microscopy. The number of vesicles over time in each cell, or the average number of vesicles/cell are plotted (error bars represent SEM). A representative movie is shown of n=3 separate experiments. Boxed regions are shown magnified as individual stills. Scale bars 20 μ m and 5 μ m in magnified stills. (F) HUVEC were transiently transfected with Quad-K Jam-C-HRPout, fixed and incubated with diaminobenzidine and hydrogen peroxide for 30 min. Cells were then secondarily fixed and 70 nm sections prepared and imaged by transmission electron microscopy. Precipitated DAB can be clearly seen on early endosomes but there is little evidence of labelling on multi-vesicular bodies (a, b and c) Scale bar 200 nm.

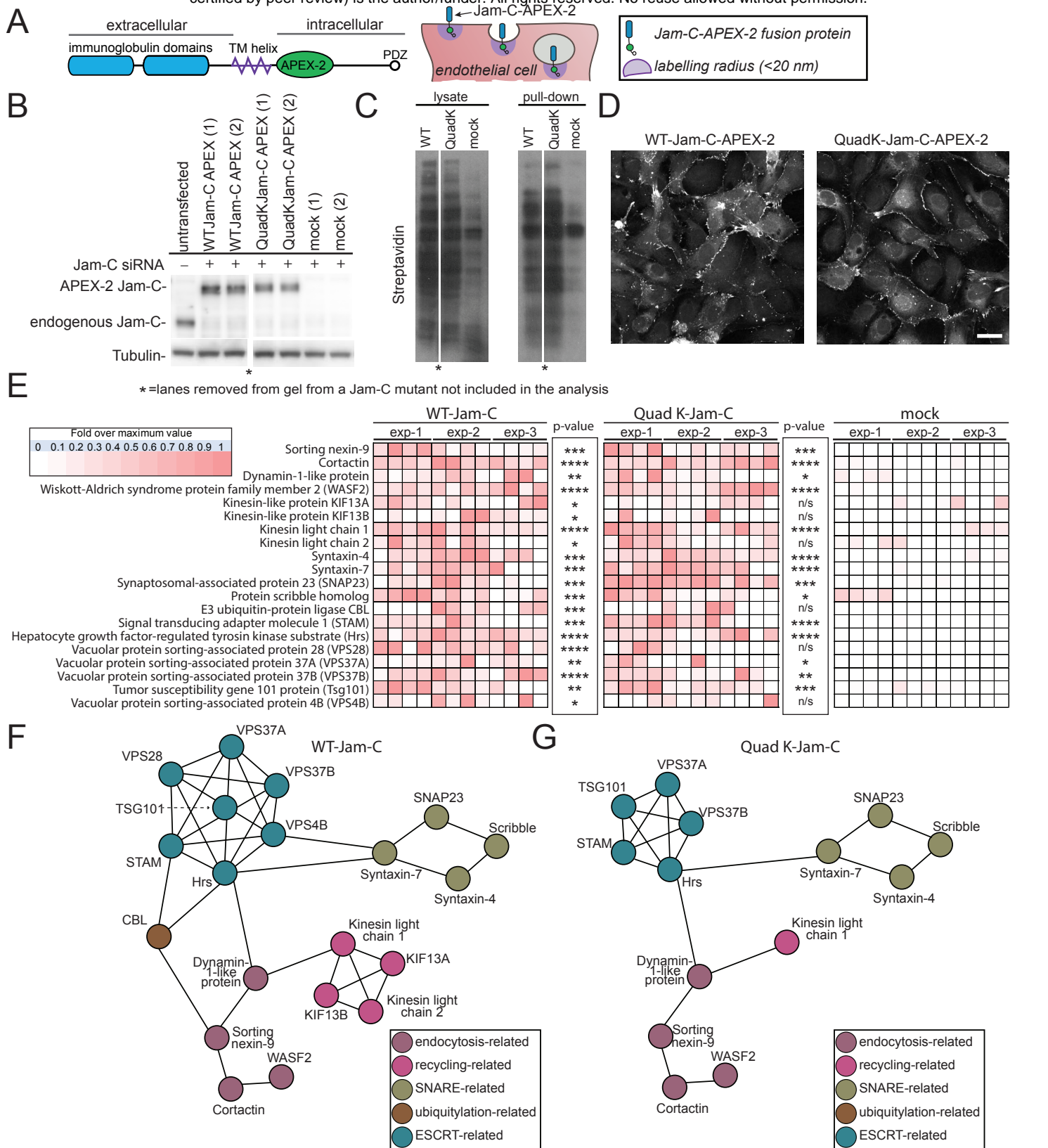


Figure 6 An APEX-2 proximity labelling approach reveals potential Jam-C trafficking machinery.

(A) Schematic of the domain structure of the Jam-C-HRP-APEX-2in construct showing the extracellular immunoglobulin domains (blue), the APEX-2 tag (green oval) and the intracellular PDZ interacting domain (clear circle). The APEX-2 tag following feeding with biotin tyramide and incubation with hydrogen peroxide for 1 min labels all neighbouring proteins within 20 nm on electron rich amino acids (purple circle). (B-E) HUVEC were transfected with WT or Quad-K Jam-C-APEX-2in. Cells were fed biotin tyramide for 30 min and then exposed to hydrogen peroxide for 1 min. The reaction was then quenched and the cells either (D) fixed and stained with streptavidin and analysed by confocal microscopy (B,C & E) lysed and biotinylated proteins pulled down using neutravidin beads for analysis by (B & C) SDS PAGE and western blot for the presence of (B) Jam-C and tubulin or (C) biotinylated proteins or (E) following an on bead tryptic digest, mass spectrometry. A heat map of $n=3$ independent mass spectrometry data sets is shown with white representing no signal and dark red a high signal. Each individual experiment was carried out in duplicate with each mass spectrometry run being repeated twice (to give a total of 4 analyses/experiment). P values are given across all 3 experiments (* $P\leq 0.05$, ** $P\leq 0.01$, *** $P\leq 0.001$, **** $P\leq 0.0001$; t test). (F & G) String analysis of proteins neighbouring (F) WT or (G) Quad-K Jam-C APEX-2 proteins. *lane removed of a Jam-C mutant not included in this analysis.

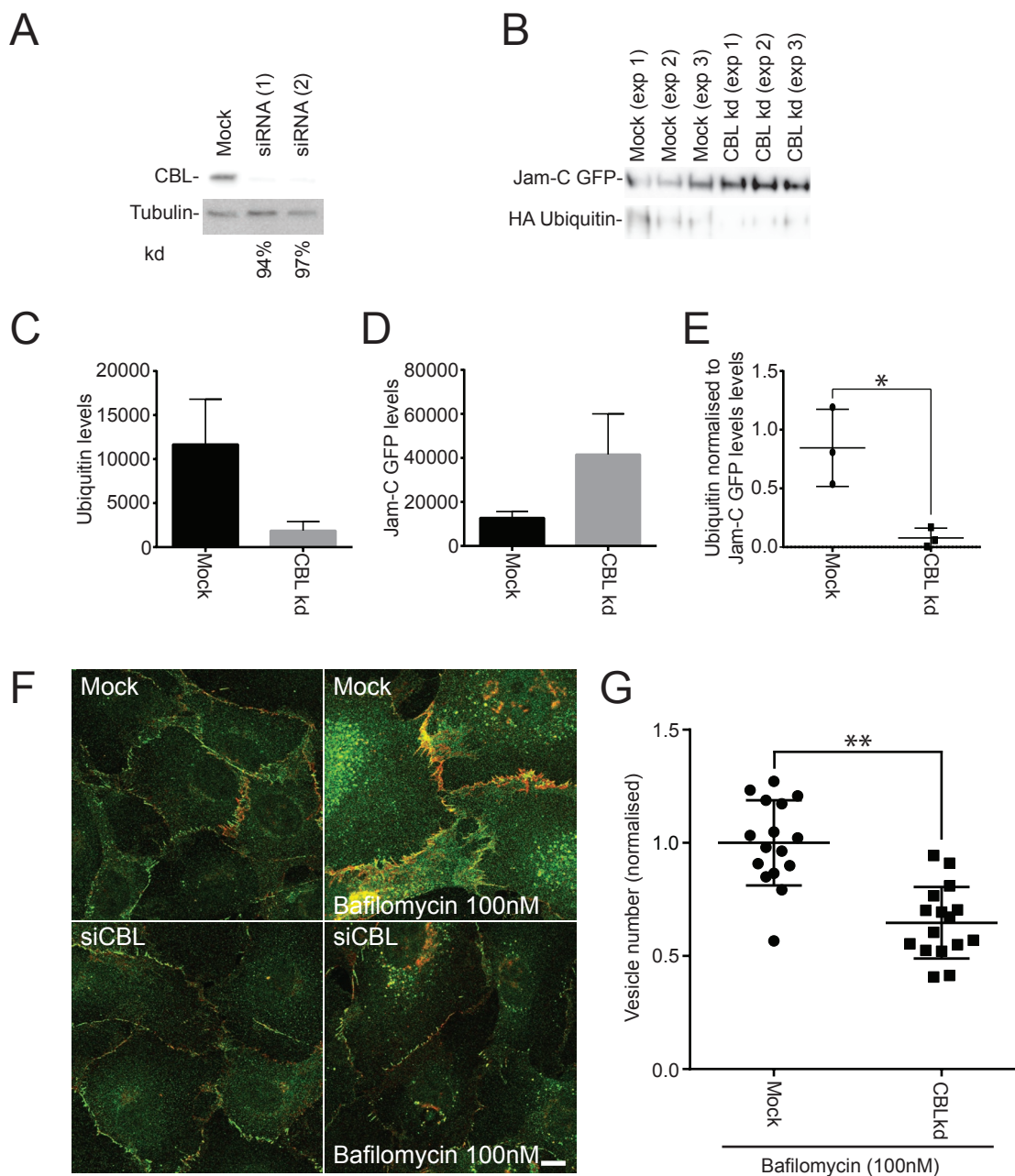


Figure 7 Jam-C is ubiquitylated by the E3-ligase CBL.

(A-G) HUVEC were transfected with two different CBL siRNA over a 96 h period. (A) Cells were lysed and analysed by SDS PAGE and western blot detecting CBL and tubulin. Knock down was typically $\geq 90\%$. (B) Untreated or CBL knock down cells were transfected with Jam-C-GFPout and HA ubiquitin. Cells were lysed and GFP tagged proteins were pulled down using GFP trap agarose beads. (C-E) Pulldown proteins were analysed by SDS PAGE and western blotted for the presence of GFP and HA tagged proteins. Quantification of (C) HA ubiquitin levels (D) Jam-C-GFPout levels or (E) Ubiquitin levels normalised to levels of Jam-C. Results are from $n=3$ experiments. Error bars represent SEM ($*P \leq 0.05$; t test). (F) Mock and CBL knockdown cells were incubated with and without 100nM Bafilomycin for 4 h and then fixed and labelled for endogenous VE-Cadherin (red) and Jam-C (green). (G) Quantification of the number of Jam-C positive vesicles present in mock and CBL knock-down cells treated with 100 nM bafilomycin (5 fields of view/condition). Results are shown normalised to the mean number of vesicles in the mock cells from $n=3$ experiments. Error bars represent SD ($**P \leq 0.01$; t test).

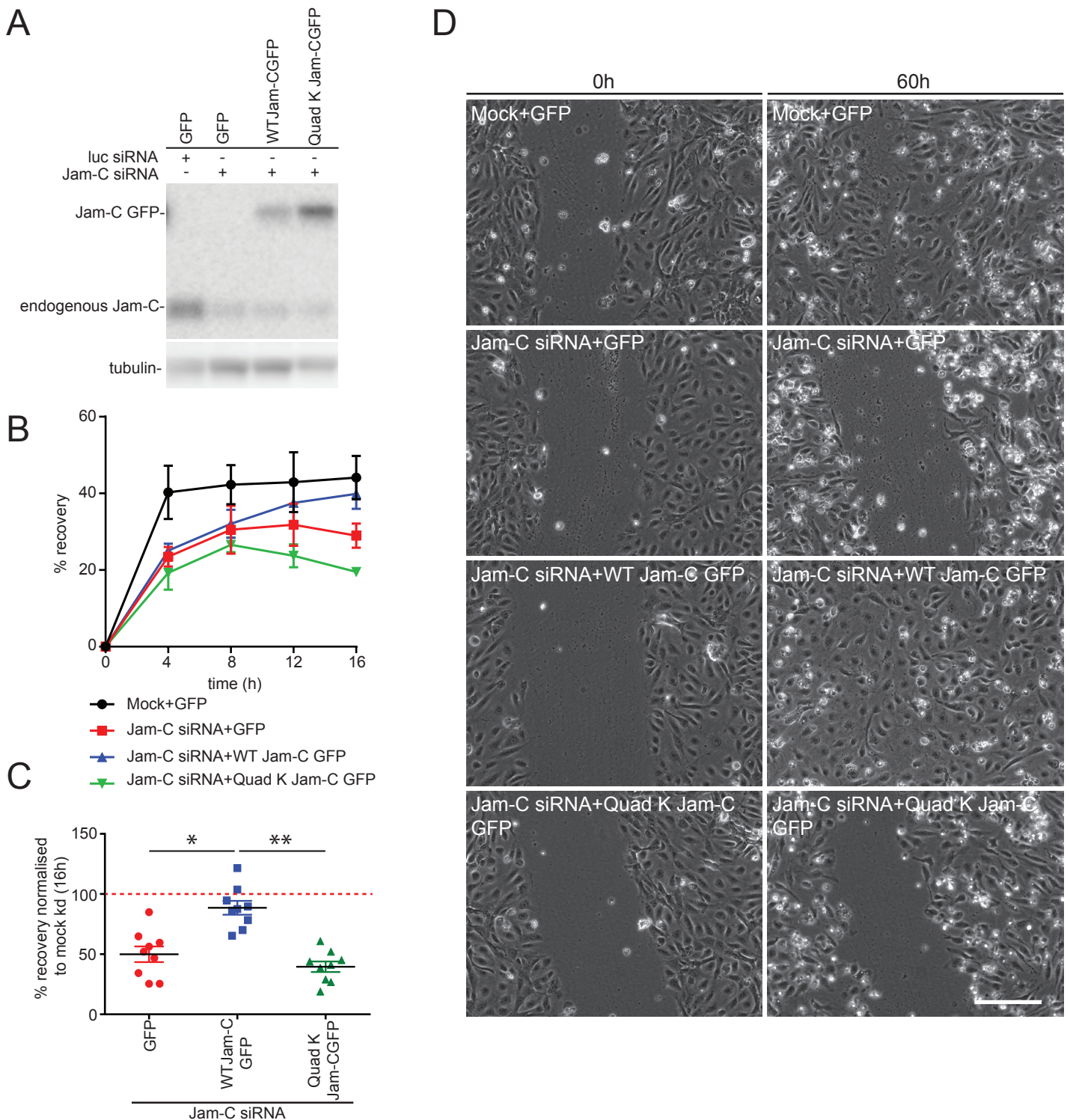


Figure. 8 Ubiquitylation of Jam-C is required for HUVEC migration.

(A-D) HUVEC were transfected with siRNA targeting luciferase or Jam-C over a 96h period. The day after the second round of transfection cells were additionally transduced with either a GFP, WT Jam-C-GFPout or a Quad K Jam-C-GFPout expressing lentivirus and allowed to reach confluency. (A) Cells were lysed and the extent of Jam-C knock down and rescue determined by western blot relative to a tubulin loading control. The expressed WT and Quad K constructs were similar to endogenous levels. (B-D) The monolayer was scratched and the cells allowed to recover over a 0-60 h time period whilst being imaged on a brightfield Olympus microscope. (B) A representative experiment showing the percentage recovery of cells over a 16 h time period. Mock treated cells expressing the GFP construct recover relatively quickly. Jam-C siRNA treated cells fail to recover when rescued by transduced QuadK Jam-C-GFPout or GFP construct. However, almost complete recovery is apparent using transduced WT Jam-C-GFPout construct after 16 h. Error bars represent standard deviation. (C) The percentage recovery of siRNA treated GFP, WT Jam-CGFP or QuadK Jam-CGFP transduced cells at 16 h is shown normalised to the mock/GFP rescued condition. Data shown from n=4 experiments, error bars represent SEM (* $P \leq 0.05$, ** $P \leq 0.01$; unpaired t-test). (D) Representative images of recovery of scratch wounds after 60 h. Scale bar 200 μm .

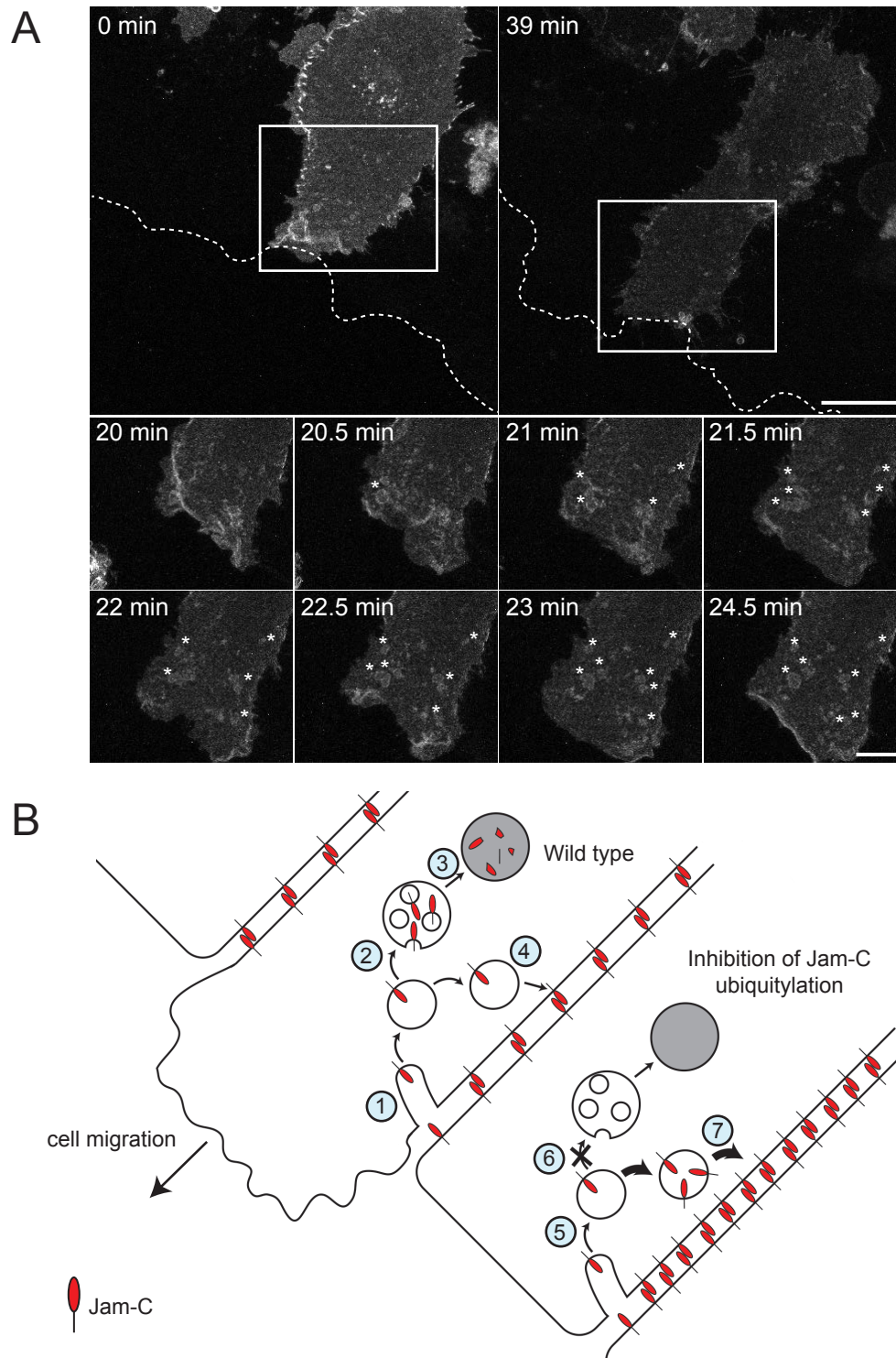
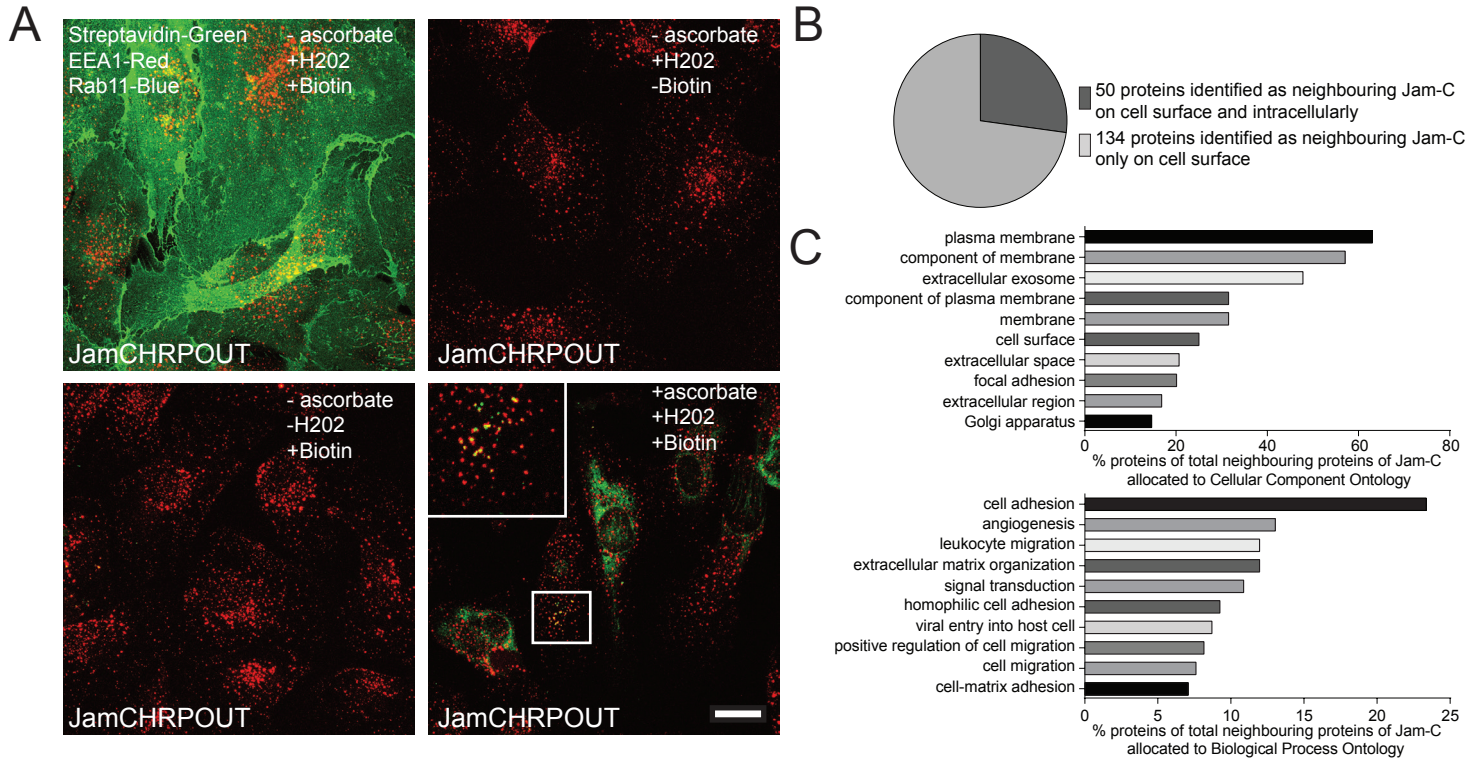


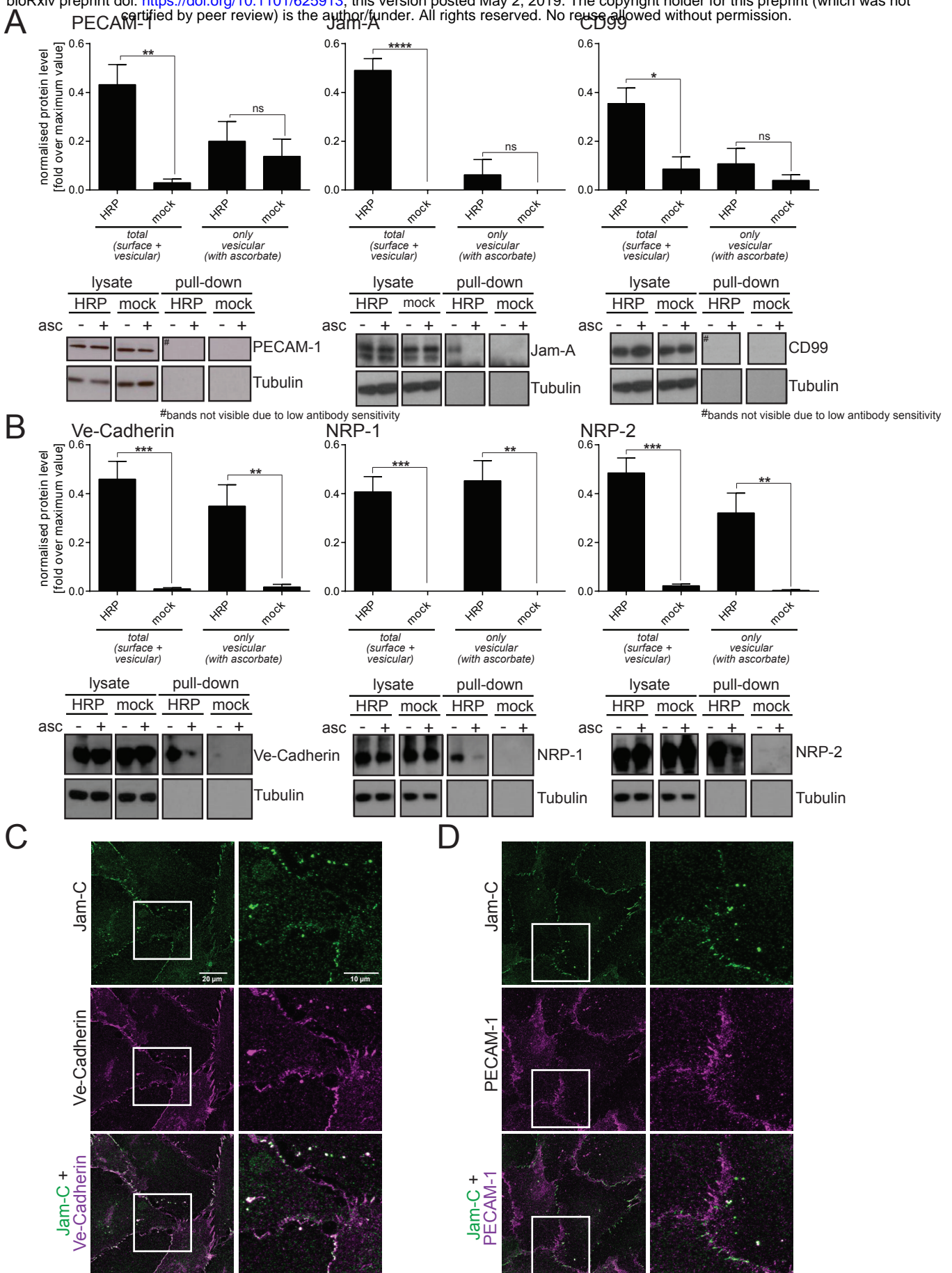
Figure. 9 Jam-C is internalised from junctions near the front of migrating cells.

(A) Jam-C-GFPout was expressed in HUVEC and the cells allowed to form a confluent monolayer. The cell layer was scratched and 45 min later live cell imaging was carried out with images acquired every 30 s for 40 min. The dotted line represents the edge of the scratch wound (as determined by DIC imaging), asterisks highlight vesicles and the boxed region is shown magnified. Scale bar 20 μ m in original images and 10 μ m in magnified images. (B) Model of the role of Jam-C trafficking in endothelial cell migration. **Wild type**: (1) Jam-C is endocytosed from the junction either side of the leading edge and is localised to endosomes. (2) As Jam-C enters endosomes the E3 ligase CBL ubiquitylates the cytoplasmic tail on lysine residues, allowing recruitment of the ESCRT complex and the formation of intra-luminal vesicles. (3) Jam-C is degraded in the lysosomes preventing excessive recycling and/or abrogating signalling. (4) The remaining Jam-C that is not ubiquitylated is recycled to the cell surface to reform new junctions after the cell has moved. **Inhibition of Jam-C ubiquitylation**: (5) Jam-C is endocytosed from the junction either side of the leading edge and is localised to endosomes. (6) Mutation of Jam-C or absence of CBL prevents ubiquitylation and recruitment to the intraluminal vesicles of late endosomes. (7) Failure to degrade Jam-C results in an increased premature recycling of Jam-C to the cell junction resulting in greater adhesion between cells and/or enhanced signalling.



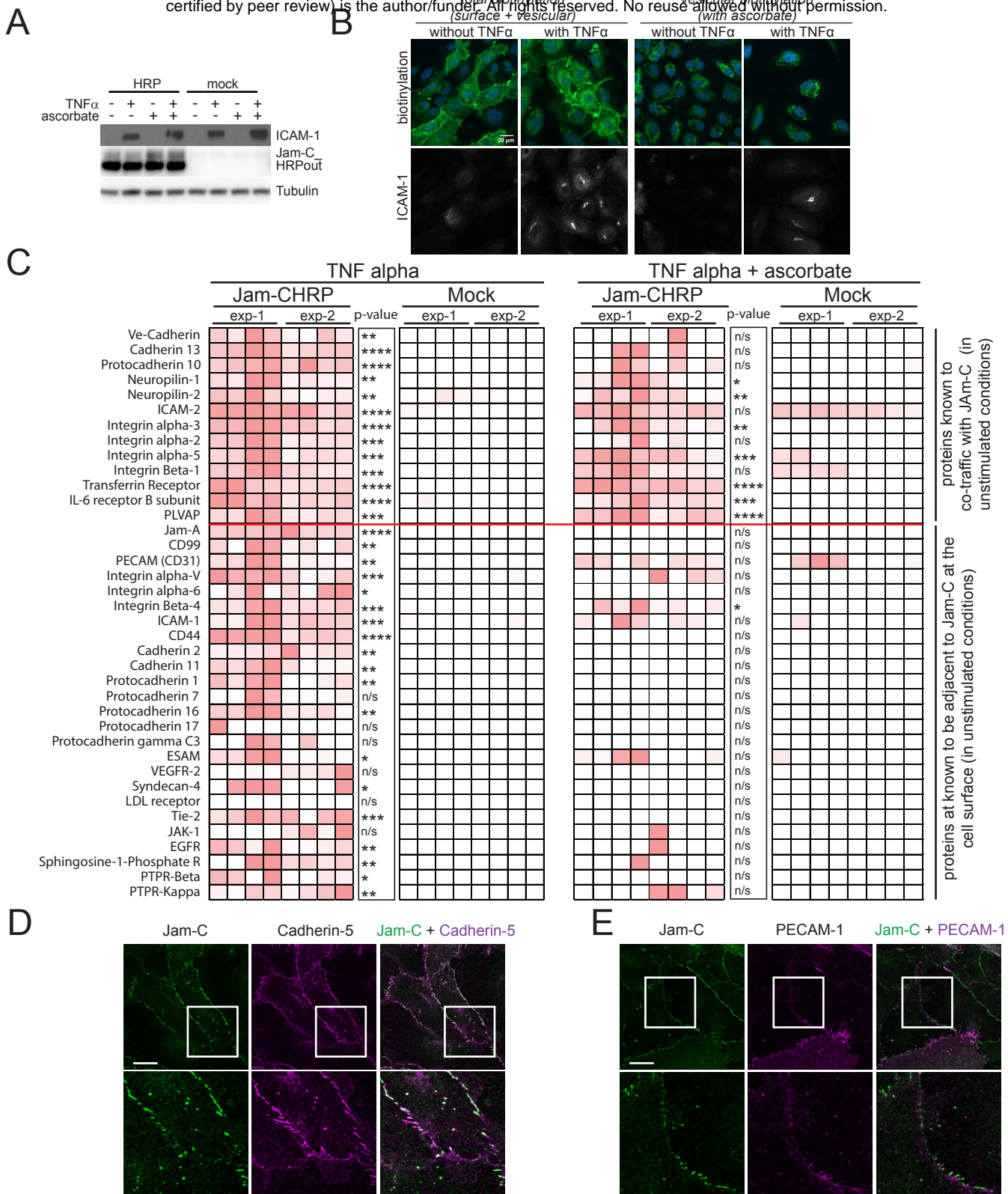
Supplementary Figure. 1 The Jam-C HRP biotinylation assay.

(A-C) HUVEC were transfected with Jam-C HRP and the following day incubated with or without biotin tyramide and hydrogen peroxide in the presence or absence of 50 mM ascorbate. (A) Immunofluorescence analysis of cells labelled for Streptavidin (Green) and early endosome antigen 1 (EEA 1, Red). Biotinylated proteins are only present when both hydrogen peroxide and biotin tyramide is present and partially localise with early endosomes. (B-C) Biotinylated proteins were pulled down with streptavidin and analysed by mass spectrometry (n=4 experiments) (B) Pie chart showing the number of proteins adjacent to Jam-C at the cell surface and intracellularly. (C) The percentage of protein hits associated with specific cellular locations and processes is plotted.



Supplementary Figure. 2 Validation of HRP biotinylation assay by western blot and Immunofluorescence analysis.

(A & B) Jam-C-HRPout transfected cells were fed with biotin tyramide and exposed to hydrogen peroxide in the presence or absence of ascorbate. Biotinylated proteins were pulled down and western blotted for (A) proteins neighbouring Jam-C at the cell surface: PECAM-1, Jam-A and CD99 or (B) proteins co-trafficked with Jam-C: VE-Cadherin, NRP-1 and NRP-2. Representative blots are shown with quantification of n=4 experiments, error bars represent SEM (* $P \leq 0.05$, ** $P \leq 0.01$; *** $P \leq 0.001$, **** $P \leq 0.0001$; unpaired t-test). (C) Immunofluorescence analysis of endogenous Jam-C (green) and either VE-Cadherin or PECAM-1 (magenta). The boxed region is magnified. VE-Cadherin co-trafficks with Jam-C whilst PECAM-1 does not.



Supplementary Figure. 3 An HRP based proximity labelling approach reveals changes in Jam-C co-trafficking following stimulation with TNF α .

(A-C) HUVEC were transfected with Jam-CHRP out and stimulated for 4 h with 50 ng/ml TNF α . (A) Cells were lysed and analysed by western blot. The level of Jam-C HRP expression is similar across all transfected samples and TNF α stimulation upregulates the expression of ICAM-1. (B & C) Cells were fed biotin tyramide for 30min and then exposed to hydrogen peroxide for 1min in the presence or absence of 50mM ascorbate. (B) Cells fixed and stained with streptavidin (green), DAPI (blue) and ICAM-1 (grey). Images were acquired by confocal microscopy. Scale bar 20 μ m. (C) Biotinylated proteins were pulled down using neutravidin beads and pulldown samples were analysed by mass spectrometry. Heat map of 2 independent mass spectrometry data sets is shown with white no signal and dark red a high signal. Each individual experiment was carried out in duplicate with mass spectrometry runs being repeated twice (to give a total of 4 analyses/experiment). P values are given across 2 experiments (*P \leq 0.05, **P \leq 0.01, ***P \leq 0.001, ****P \leq 0.0001; t-test). Co-trafficked proteins appear in both +/- ascorbate conditions whilst proteins adjacent to Jam-C solely at the cell surface are only present in the - ascorbate condition. (D & E) HUVEC were stimulated for 4 h with TNF α fixed and labelled for (D) Jam-C (Green) and VE-Cadherin (magenta) or (E) Jam-C (Green) and PECAM-1 (Magenta). Jam-C does not co-localise with VE-Cadherin or PECAM-1. Scale bar 20 μ m.

715 **Primers for Mutagenesis**

Mutant	Primer	Sequence (5'-3')
Y267A	F	GGCATCTGCTGTGCGGCCAGACGAGGCTGCTTC
	R	GAAGCAGCCTCGTCTGGCCGCACAGCAGATGCC
S281A	F	CAGTAAACAAGATGGAGAAGCCTATAAGAGCCCAGGGAAGC
	R	GCTTCCCTGGGCTCTTATAGGCTTCTCCATCTTGTTTACTG
Y282A	F	GTAAACAAGATGGAGAAAGCGCTAAGAGCCCAGGGAAGCATGAC
	R	GTCATGCTTCCCTGGGCTCTTAGCGCTTTCTCCATCTTGTTTAC
K283R	F	GATGGAGAAAGCTATAGGAGCCCAGGGAAGCATG
	R	CATGCTTCCCTGGGCTCCTATAGCTTTCTCCATC
K287R	F	CTATAAGAGCCCAGGGAGGCATGACGGTGTTAAC
	R	GTTAACACCGTCATGCCTCCCTGGGCTCTTATAG
Y293A	F	GCATGACGGTGTTAACGCCATCCGGACGAGTGAGG
	R	CCTCACTCGTCCGGATGGCGTTAACACCGTCATGC
T296A	F	GGTGTTAACCTACATCCGGGCGAGTGAGGAGGGTGACTTCAG
	R	CTGAAGTCACCCCTCCTCACTCGCCCGGATGTAGTTAACACC

716

717 **Infusion replacement of HRP for GFP in Jam-C GFP Out**

Protein	Primer	Sequence (5'-3')
HRP	F	GGAAGTCTATTCTAGAATGCAGTTAACCCCTACATTCTAC
	R	CCAGCAATGTTCAACTCGAGAGAGTTGCTGTTGACCACTCTG

718

719 **Infusion subcloning of Jam-C GFP Out into lentiviral vectors**

Mutant	Primer	Sequence (5'-3')
WT Jam-C GFP Out	F	GGATCCCGGGCTCGAGATGGCGCTGAGCCGGCG
	R	TACCAGGCCTCTCGAGTCAGATAACAAAGGACGATTTGTGT
Quad K Jam-C GFP Out	F	GGATCCCGGGCTCGAGATGGCGCTGAGCCGGCG
	R	TACCAGGCCTCTCGAGTCAGATAACAAAGGACGATCTG

720 **Supplementary Table 1. Primer Sequences**

Antibody	Source	Cat #/Ref	Species	Details
HA	Roche	118674230 01	Rat monoclonal	Western 1:250
GFP	Chromotek	3H9	Rat monoclonal	Western 1:1000
Jam-C	A kind gift from Prof Beat Imhof (University of Geneva)	J81	Western 1:1000 IF 1:1000	Western 1:1000 IF 1:1000
Jam-C	Bethyl Laboratories	A303-761A	Rabbit polyclonal	Western 1:1000
VE-cadherin	Santa Cruz	Sc9989	Mouse monoclonal	Western 1:1000 IF 1:100
ZO-1	Cell signalling technology	D6L1E	Rabbit monoclonal	Western 1:1000 IF 1:100
CD63	AbCAM	CLB180	Mouse monoclonal	IF 1:100
Rab11	Lifetechnologies	71-5300	Rabbit polyclonal	IF 1:100
NRP-1	AbCAM	Ab81321	Rabbit polyclonal	Western 1:1000 IF 1:100
NRP-2	R &D Signalling	AF2215	Rabbit polyclonal	Western 1:200 IF 1:50
PECAM (CD31)	E-bioscience	17-0319-41	Mouse monoclonal (WM-59)	IF 1:200
PECAM (CD31)	Santa Cruz	Sc1506	Goat polyclonal	Western 1:1000
Jam-A	Santa Cruz	Sc53628	Mouse monoclonal	Western 1:1000 IF 1:100
CD99	Santa Cruz	Sc28389	Mouse monoclonal (12E7)	Western 1:100
Tubulin	Sigma	T4026	Mouse monoclonal (Tub2.1)	Western 1:1000
Streptavidin HRP	DAKO	P0397	-	Western 1:1000
ICAM-1	Santa Cruz	Sc7891	Rabbit polyclonal	Western 1:1000
CBL	Santa Cruz	Sc398282	Mouse monoclonal	Western 1:1000

721 Supplementary Table 2. **Antibodies**